UNIVERSITÀ DI PARMA
ARCHIVIO DELLA RICERCA

University of Parma Research Repository

Recharge, groundwater flow pattern and contamination processes in an arid volcanic area: Insights from isotopic and geochemical tracers (Bara aquifer system, Republic of Djibouti)

This is the peer reviewd version of the followng article:

Original
Recharge, groundwater flow pattern and contamination processes in an arid volcanic area: Insights from isotopic and geochemical tracers (Bara aquifer system, Republic of Djibouti) / Awaleh, Mohamed Osman; Baudron, Paul; Soubaneh, Youssouf Djibril; Boschetti, Tiziano; Hoch, Farhan Bouraleh; Egueh, Nima Moussa; Mohamed, Jalludin; Dabar, Omar Assowe; Masse Dufresne, Janie; Gassani, Jean. - In: JOURNAL OF GEOCHEMICAL EXPLORATION. - ISSN 0375-6742. - 175:(2017), pp. 82-98. [10.1016/j.gexplo.2017.01.005]

Availability:
This version is available at: 11381/2820477 since: 2018-09-17T15:04:11Z

Publisher:
Elsevier B.V.

Published
DOI:10.1016/j.gexplo.2017.01.005

Terms of use:

Anyone can freely access the full text of works made available as "Open Access". Works made available

Publisher copyright

note finali coverpage

(Article begins on next page)

02 May 2026

Accepted Manuscript

Recharge, groundwater flow pattern and contamination processes in an arid volcanic area: Insights from isotopic and geochemical tracers (Bara aquifer system, Republic of Djibouti)

Mohamed Osman Awaleh, Paul Baudron, Youssouf Djibril Soubaneh, Tiziano Boschetti, Farhan Bouraleh Hoch, Nima Moussa Egueh, Jalludin Mohamed, Omar Assowe Dabar, Janie Masse-Dufresne, Jean Gassani

PII: S0375-6742(17)30018-3
DOI: doi: 10.1016/j.gexplo.2017.01.005
Reference: GEXPLO 5885

To appear in: *Journal of Geochemical Exploration*

Received date: 27 June 2016
Revised date: 30 November 2016
Accepted date: 6 January 2017

Please cite this article as: Mohamed Osman Awaleh, Paul Baudron, Youssouf Djibril Soubaneh, Tiziano Boschetti, Farhan Bouraleh Hoch, Nima Moussa Egueh, Jalludin Mohamed, Omar Assowe Dabar, Janie Masse-Dufresne, Jean Gassani , Recharge, groundwater flow pattern and contamination processes in an arid volcanic area: Insights from isotopic and geochemical tracers (Bara aquifer system, Republic of Djibouti). The address for the corresponding author was captured as affiliation for all authors. Please check if appropriate. Gexplo(2017), doi: 10.1016/j.gexplo.2017.01.005

This is a PDF file of an unedited manuscript that has been accepted for publication. As a service to our customers we are providing this early version of the manuscript. The manuscript will undergo copyediting, typesetting, and review of the resulting proof before it is published in its final form. Please note that during the production process errors may be discovered which could affect the content, and all legal disclaimers that apply to the journal pertain.

ACCEPTED MANUSCRIPT

Recharge, groundwater flow pattern and contamination processes in an arid volcanic area: insights from isotopic and geochemical tracers (Bara aquifer system, Republic of Djibouti)

Mohamed Osman Awaleh[a*], Paul Baudron[b,c,d], Youssouf Djibril Soubaneh[e], Tiziano Boschetti[f], Farhan Bouraleh Hoch[a], Nima Moussa Egueh[a], Jalludin Mohamed[a], Omar Assowe Dabar[a], Janie Masse-Dufresne[b], Jean Gassani[a]

[a]Institut des Sciences de la Terre. Centre d'Etudes et de Recherches de Djibouti (CERD). Route de l'aéroport. B.P. 486. Djibouti – ville. République de Djibouti.

[b]Département des génies civil, géologique et des mines, Polytechnique Montréal C.P. 6079. succ. Centre-Ville. Montréal. Qc. Canada. H3C 3A

[c]UMR G-EAU, BP 5095, 34196 Montpellier Cedex 5, France

[d]GEOTOP Research Center, Montréal, Canada

[e]Département de biologie, chimie et géographie. Université du Québec à Rimouski. 300. Allée des Ursulines. Rimouski. QC. G5L 3A1. Canada.

[f]Department of Physics and Earth Sciences "Macedonio Melloni", University of Parma, Parco Area delle Scienze 157/a 43124 Parma – Italy.

Abstract

Fractured volcanic aquifers are the main water resources in the arid climate of the Republic of Djibouti. Nonetheless, these strategic reservoirs are overexploited and their comprehensive understanding is therefore a pre-requisite for a sustainable use. A geochemical and isotopic survey, including major ion chemistry, ^{2}H, ^{18}O, ^{13}C, ^{3}H, $^{87}Sr/^{86}Sr$, ^{15}N was performed and

ACCEPTED MANUSCRIPT

combined with existing ^{14}C data to study recharge, contamination processes and groundwater flow patterns inside and between the compartments of a complex aquifer system composed by basaltic rocks and by alluvium located in Petit Bara, Grand Bara, and Mouloud areas (Southwest of Djibouti). A main feature was the common trend from a fresh Na-Cl-HCO_3 water type (alluvium groundwaters) to an intermediate water type (alluvium and basalt groundwaters) and finally to a Na-Cl-SO_4 water type (most mineralized basalt groundwater). Elementary and isotopic nitrate evidenced and located anthropogenic and geogenic origins of nitrate. Alluvium groundwaters had δ^2H and $\delta^{18}O$ signature of modern precipitation while basalt groundwaters were significantly depleted and enriched in $\delta^{13}C$ due to water-rock interactions. Modern radiocarbon and tritium were evidenced in the alluvium groundwaters, while recalculated radiocarbon ages located recharge of the basalt groundwaters in the early to mid-Holocene. These features revealed a common evolutionary pattern, with a recharge from wadi-rivers to the alluvium and a downward circulation to the basalt through major faults, combined with a mixing with a more geochemically evolved groundwater. Accordingly, highly saline groundwater at the outlet of the Petit Bara plain was found to be diluted by modern recharge in the alluvium. Two major basaltic aquifer compartments were found to be connected (Grand Bara and Mouloud), revealing a global northeastward flowpath below the endorheic Grand Bara plain.

Keywords: Djibouti, Hydrochemistry, Volcanic aquifer, Stable isotopes, Nitrogen isotopes

*Corresponding author. Tel: +253 77 84 68 55; Fax: +253 21 35 45 68; awaleh@gmail.com

ACCEPTED MANUSCRIPT

1. Introduction

The republic of Djibouti (23,000 km^2) is located in the Horn of Africa (Fig. 1), which is an emerged triple junction of the Red Sea, the Gulf of Aden and the East African Rift that correspond to large seismic, tectonic and volcanic activities (Barberi et al., 1975; Mlynarski and Zlotnicki, 2001).

On the other hand, the republic of Djibouti is subjected to an arid climate with an annual mean rainfall of 150 mm. This harsh climate explains the lack of permanent rivers, and has led the country to exploit the only available water resources, which are represented by groundwater in the volcanic aquifers (Jalludin and Razack, 1994). The continuous and drastic increases in water demand has led to an intensive exploitation of volcanic aquifers and has severely depleted its reserves and led to quality deterioration (Houssein and Jalludin, 1996), as found in several arid to semi-arid aquifers worldwide (e.g. Jimenez-Martinez et al., 2016).

The population of Djibouti relies heavily on groundwater resources for drinking water and irrigation purposes. Therefore, knowledge of the origin of groundwater resources and their renewal forms as well as the consideration of their vulnerability facing the anthropogenic pressure is essential to the rational management of volcano-sedimentary aquifers in Djibouti. However, few studies have been carried out on the hydrogeology (Jalludin and Razack, 1994; Jalludin and Razack, 2004) and hydrochemistry (Aboubaker et al., 2013) of these complex volcano-sedimentary aquifers. These studies address only briefly recharge conditions, groundwater residence times and groundwater flow pattern inside these aquifer systems. In order to fulfill this gap, environmental and radiogenic isotopes (δ^2H, $\delta^{18}O$, ^3H, $\delta^{13}C$, ^{14}C, $^{87}Sr/^{86}Sr$) as well as major ion chemistry combined with hydrogeological and geological data are applied to

ACCEPTED MANUSCRIPT

assess groundwater dynamics of the Bara aquifer systems located on the north of the East Africa Rift.

Furthermore, nitrate dual isotopes ($\delta^{15}N–NO_3^-$ and $\delta^{18}O–NO_3^-$) are applied to identify the major sources of NO_3^- in groundwaters from this volcano-sedimentary aquifer. Indeed, the isotopic composition of dissolved nitrate in waters ($\delta^{15}N–NO_3^-$ and $\delta^{18}O–NO_3^-$) has been used extensively to better constrain the sources of nitrate in groundwater (Edmunds and Gaye, 1997; Jackson et al., 2015; Kendall, 1998; Kendall et al., 2007; Stadler et al., 2008; Walvoord et al., 2003). However, to the best of our knowledge, no nitrate dual isotopes were used to investigate the origin of nitrate in groundwater in arid or semi-arid rift systems. The present study reports the first results of nitrogen isotopes of groundwater from semi-arid environment located in the East Africa Rift.

The results of this study will contribute to a comprehensive knowledge of the complex volcano-sedimentary aquifer systems in the Bara basin, by defining the groundwater flow pattern and the relations between aquifer compartments, assessing groundwater residence time and deciphering the origin of high nitrate content in semi-arid environment in the East Africa Rift areas. This study would serve as a valuable base for other integrated hydrodynamic, geochemical and isotopic studies of volcano-sedimentary aquifers in similar arid environments.

2. Site description

2.1 Climate and hydrology

The republic of Djibouti has a low precipitation regime, with annual mean rainfall of 150 mm. Overall, two seasons predominate: a cool season (winter) from October to April and a hot season (summer) from May to September. In winter, the climate is characterized by northeast trade

ACCEPTED MANUSCRIPT

winds coming from Saudi and Gulf of Aden and mean temperature comprised between 20ºC and 30ºC. In summer dominates equatorial westerly wind zone and mean temperatures comprised between 30ºC and 45ºC with high rate of evapotranspiration amounting to 2000 mm per year (BGR, 1982).

The study area is localized in two main surface watersheds, which are Grand Bara and Ambouli (Fig. S1, see supporting information). The Grand Bara watershed, with an area of 869 km², is characterized by an average altitude of 630 meters and average slopes of 9%. Due to the low permeability of outcropping rocks, this endorheic basin plays a major role in the concentrated runoff process and flash flood of different wadis to its localized downstream portion in the center of this depression. The Ambouli surface watershed, with an area of 774 km² and an average altitude of 470 meters and average slopes of 10%, is an exoreic watershed with its outlet in Djibouti city. The Petit Bara area (140 km²) is located in the upstream part of the Ambouli surface watershed.

2.2 Geological settings

The Republic of Djibouti is located in the Southeastern part of the Afar rift which resulted from the intersection of two nascent mid-oceanic ridges (Red Sea and Gulf of Aden) and a continental rift (East African Rift) during the Miocene (Fig. 1). The first evidence of synrift magmatism in SE Afar is the 28–19 Ma Ali Sabieh mafic complex located in the South of the country and the more widespread Mablas rhyolites. These basalts are the effusive component of a magmatic complex that includes a laccolithic intrusion, the emplacement of which is assumed to have caused the NE-plunging antiform structure of the Ali Sabieh ranges by arching the Mesozoic sedimentary rocks (Le Gall et al., 2010). The Mablas rhyolites form the outer rim of this antiform and consist of rhyolites, ignimbrites and minor basaltic lava flows, intruded by felsic dykes

ACCEPTED MANUSCRIPT

(Gadalia, 1980; Audin et al., 2004). These rhyolites were followed by the emplacement of the Dalha series, in which about 1000 m of basaltic flows erupted at 8.3-4.3 Ma, just before the initial opening of the Tadjoura Gulf (Gasse et al., 1986). These basalts are correlative with the Somali basalts emplaced approximately during the same period of time (7.2-3 Ma) (Audin et al., 2004).

Gasse et al. (1986) are reported for the Dalha series an aphyric facies with plagioclase olivine and pyroxene minerals. In addition, sedimentary rocks (clays, alluviums, diatomites) interbedded in Dalha basalts and fill tectonic basins.

The Stratoid basalts (3-1 Ma) cover two-third of the Afar depression. They unconformably overlie the Dahla basalts series and the sedimentary formation. During the last 3 Ma, the SE Afar margin recorded several episodes of extensional faulting in various tectonic setting (Daoud et al., 2011).

The study area is located in the south-eastern part of the country. The Petit Bara and Grand Bara zones correspond to sedimentary basins limited to the East by the Dalha basalts (8.3-4.3 Ma) and to the West by the Stratoid basalts (3-1 Ma) (Fig. 1).

The Petit Bara and the Grand Bara zones describe clearly different fracture trends of the Dalha basalts (Arthaud and Jalludin, 1993). A common zone separates both plains and shows a relatively regular fault network with EW and N160°-180° fractures. All the western part of the Grand Bara plain is characterized by mainly EW and N110°-130° faults (Arthaud and Jalludin, 1993). Dalha basalts fractures have a particular behavior with elliptical faults lines in the Northern part of the Petit Bara (Arthaud and Jalludin, 1993).

The #1 – #6 boreholes are located mainly in the Didjan Der valley at the north of the Petit Bara area, while #7 borehole is drilled in the south-east of the Petit Bara plain (Fig. 1). The depth of these boreholes ranges from 92 and 170 meters (Table 1). The lithologies of the #2 – #5 boreholes consist of alluvia and altered scoria interbedded with clays, this latter is associated with

ACCEPTED MANUSCRIPT

calcite, while the ≠6 borehole consists of alternation of basalts, alluvia interbedded with silts and calcareous clays.

It is of interest to note that the ≠8 borehole was located on the basalt outcrop between the Petit Bara zone and the Grand Bara zone. That is why we have categorized ≠8 borehole as Central area in the Table 1. Since we didn't want to classify this central area apart, we decided to put ≠8 borehole in the Petit Bara zone in the Table 1.

In the Grand Bara zone, the study area is focused on the western flank of the Dalha basalts (#9, #11, #13, #14, #15, #16 and #17 boreholes); whereas only one borehole (#18) is located in eastern part of the Stratoid basalts, while borehole #12 is located in the Grand Bara plain. In this area, the Dalha basalts are affected by two distinct sets of faults at N160-180°E croscutted by E-W faults-fractures and to a lesser extent N110 -130°E croscutted by NS and N60-70°E directions. The basalts are delimited by several wadi valleys (Dagahdamer, Awraoussa, Dadin, and Mouloud). Depth of the drilled boreholes ranges between 90 and 181 meters, except for the #13 shallow dugwell which has a depth of about 19 m (Table 1). The following vertical successions were observed: (1) alternation of calcareous silts, sands, alluvia and clayish silts (#10); (2) calcareous sands and alluvium interbedded with altered basalts and scoria (#17); and finally (3) alternation of sands, alluvia associated with pebbles of basalts and rhyolites, silts, altered basalts and scoria (#15 and #16).

The Mouloud-Dadin area, which is part of the Dikhil basin, is located between the plain of Grand Bara and Dalha basalts (Fig. 1). Depth of the drilled boreholes in this area ranges between 115 and 150 meters (Table 1). The drilled sections exhibit complex deposits with an alternation of basaltic lava flows interbedded with alluvia and argillaceous sediments for Dadin (#22). Aboubaker (2012) reported that Dalha basalts appear on approximately ten meters. The Mouloud boreholes (#20, #21) are characterized by alluvia and basalts interbedded with sedimentary rocks

ACCEPTED MANUSCRIPT

(alluvia and clays). Calcite occurs in vesicles of scoria and fissures. The alternation of alluvium, altered basalts, scoria with calcite, argillaceous sediments in the different wells hardens the correlation between them.

2.3 Hydrogeological settings

The groundwater in Djibouti is controlled by volcanic and sedimentary aquifers. Volcanic aquifers systems are mainly represented by the Dalha basalts, the stratoid basalts and the Mabla rhyolites (BGR 1982; Jalludin and Razack 1994; Jalludin and Razack 2004).

Sedimentary aquifers are located in the two plains of Petit Bara and Grand Bara and also along the main wadi beds (Fig. 1). The plains are generally filled by very heterogeneous sediments with coarse materials as gravels, sands, shales and fine sediments. The substratum is represented by the Dalha basalts. Pleistocene sediments mainly fill the plains and the upper part is irregularly covered by holocene deposits. The thickness might exceed 150 meters in "Grand Bara" and "Petit Bara" sediments should be above 100 meters. In addition, sediments along the narrow wadi bed form of a few to several tens of meters thick aquifer systems that are considered to play a significant role in the recharge mechanism. Given the geomorphological conditions and the showery type of rainfall, recharge may occur mainly in these aquifers during runoff generated by short showery periods. Recharge of the underlying Dalha basalts would then be ensured by these wadi aquifers through faults caused by intense tectonics (Aboubaker, 2012; BGR 1982). Therefore, one may possibly consider hydraulic continuity between sedimentary and volcanic systems through tectonic faults, fissured volcanic flows and horizontal levels of slag and lava breccias.

A cross section of the Petit Bara area is shown in Fig. 2A. On the other hand, the substratum of the Grand Bara sedimentary basin is supposed to consist essentially of basalts (Fig. 2B), and the

ACCEPTED MANUSCRIPT

basaltic aquifer may continue under the sedimentary cover of the Grand Bara plain (Aboubaker, 2012). Dalha basalts and sediments unconfined aquifers are considered potential aquifers for water supply in the study area. The transmissivity of Dalha basalts ranges between 1.5 10^{-4} m²/s and 2.4 10^{-3} m²/s, and for the sediments between 5.6 10^{-6}m²/s and 1.3 10^{-3} m²/s. A cross section of the Mouloud-Dadin area highlights the geometry of the alluvial aquifer, mainly determined by the fracturing system that shift the basalt panels vertically several meters by a set of normal faults (Fig. 2C). In Mouloud-Dadin area, the transmissivities range between 10^{-3} m²/s and 10^{-4} m²/s due to the presence of clay (CERD, 2014).

3. Material and methods

Twenty two borehole waters were collected in April – June 2014. Whenever possible, water level in boreholes was measured manually with a dip meter. Temperature (±0.1 ^{o}C), pH (±0.01 unit), electrical conductivity (±1µS/cm), redox potential (±0.1 mV), and Dissolved Oxygen (±0.1 mg O_2/l) were measured on site using portable instruments, i.e. CheckTemp (Hanna), pH 610 (EutechInstruments), COND 610 (Eutech Instruments), WTW multi 3410, and YSI 550A DO Instrument respectively. Each was calibrated in the field prior to sampling. Water samples were collected in polyethylene containers after filtration through 0.45 µm membrane filters. All samples used for determination of cations were acidified after collection through addition of Suprapure® HNO_3 (Merck). Analyses of anions and major cations were carried out using a Dionex ICS 3000 Ion Chromatograph calibrated through repeated analysis of five working anions and cations standards, with concentrations within the range of analyses. Analyses of boron and strontium elements were conducted using an Ultima 2 (Horiba Jobin Yvon) Inductively Couple Plasma Atomic Emission Spectrometer (ICP-AES). National Institute of Standards and

ACCEPTED MANUSCRIPT

Technology traceable commercial standards were used for quality control. These standards were analyzed to within ±3% of the known values. For the analysis of aqueous SiO_2, the water samples were diluted fivefold using deionized water to prevent SiO_2 precipitation. SiO_2 contents were determined by colorimetry and analyzed using a Jenway 6300 spectrophotometer, while HCO_3 was analyzed by titration with 0.1 M HCl. The charge balance between anions and cations ((Σ[Anions] - Σ[Cations]) / (Σ[Anions] + Σ[Cations]); concentrations in $meql^{-1}$) was assessed and analyses were accepted for deviations of less than 3%.

Additional samples of untreated waters were collected in 50 mL glass bottles (Quorpak) for analyses of stable isotopes of the water molecule (δ^2H-H_2O and $\delta^{18}O$-H_2O), in 1000 mL plastic bottles for tritium (^3H) analysis, in 1000 mL plastic bottles for carbon-13 of dissolved inorganic carbon (^{13}C-DIC) and in 250 mL plastic bottles for $^{87}Sr/^{86}Sr$. The isotope ratios of hydrogen and oxygen were analyzed in BRGM (Orleans, France) using a Finnigan MAT 252 mass spectrometer and converted in per mil delta values (δ‰) versus the Vienna Standard Mean Ocean Water (V-SMOW) standard following δ (‰) = $[(R_{sample} / R_{standard}) - 1] \times 10^3$, where R is the isotopic ratio of interest ($^2H/^1H$ or $^{18}O/^{16}O$). The average precision, based on multiple analyses of various samples and laboratory standards was ± 0.1 ‰ for $\delta^{18}O$-H_2O and ± 0.8‰ for δ^2H-H_2O. Tritium activity measurements were done in the BRGM (Orleans, France) by direct liquid scintillation counting. The detection limit was 0.6 TU (Tritium Unit with 1 TU equal to 1 tritium atom in 10^{18} hydrogen atoms).

Sr-isotopes were measured on a VG sector 54 in dynamic mode at the GEOTOP laboratory at the Université du Québec à Montreal (Canada). $^{87}Sr/^{86}Sr$ ratios were normalized to $^{86}Sr/^{88}Sr$ = 0.1194. Repeated analyses of the NIST-987 standard yielded values of 0.710294 (±0.000022, 2σ reproducibility). Furthermore, these results were corrected to the accepted value for NIST-987 of

ACCEPTED MANUSCRIPT

0.710248. The ^{13}C contents were measured using a mass spectrometer (Micromass, Isoprime model with triple universal collectors) at the GEOTOP laboratory at the Université du Québec à Montreal (Canada). ^{13}C contents are reported using conventional δ (‰) notation as a deviation from V-PDB, and the error of $\delta^{13}C$ is 0.05‰ (mean error obtained from replicate analyses). The $\delta^{15}N–NO_3^-$ and $\delta^{18}O–NO_3^-$ values were measured at the University of Waterloo Environmental Isotope Laboratory (Canada). $\delta^{15}N–NO_3^-$ values were determined using a Carlo Erba 1108 CNOS Elemental Analyzer coupled to a Fisons Instrument Isochrom-EA mass spectrometer (GV Instruments, Manchester, UK). $\delta^{18}O–NO_3^-$ values were measured by breakseal combustion using a VG PRISM Series II mass spectrometer (GV instruments, Manchester, UK). Isotopic ratios are reported in delta (δ) notation in units of per mil (‰) relative to the reference standards of atmospheric N_2 for $\delta^{15}N$ and Vienna Standard Mean Ocean Water (VSMOW) for $\delta^{18}O$. The analytical precision for $\delta^{15}N–NO_3^-$ and $\delta^{18}O–NO_3^-$ values are ±0.3‰ and ±0.8‰, respectively.

Mineral saturation indices, P_{CO2} and $\delta^{13}C$ of aqueous CO_2 were calculated by PhreeqcI software using *llnl.dat* and *iso.dat* databases (Parkhurst and Appelo 2015; Thorstenson and Parkhurst 2004).

4. Results and discussion

Samples were separated into categories according to i) the regional sub-area and possible sub-compartment considered, namely “Petit Bara”, “Grand Bara”, “Dadin” and “Mouloud” and ii) the aquifer type the borehole corresponded to, mostly “basalt” and “alluvium”. Two additional categories corresponding to boreholes lacking stratigraphic description or in specific sub-areas are proposed, namely “Grand Bara - central” (#12, located in the central Grand Bara plain) and “Petit Bara - central” (#7 and #8, located between Petit Bara and Grand Bara).

ACCEPTED MANUSCRIPT

4.1 Hydrogeochemical pattern

4.1.1 Overall geochemical evolution

The geochemistry of analyzed groundwater samples from the study area is detailed in Table 2 and classification of the waters samples in Table 1 was made according to principles of IAH (1979). According to the salinity classification of Kharaka and Hanor (2014), most of sampled groundwaters are brackish (10 g/l > TDS > 1 g/l) with the exception of several fresh waters (TDS < 1 g/l) from North of Petit Bara (#1-#4), Grand Bara (#14) and Dadin (#22). All samples are slightly alkaline (pH from 7.2 to 8.4), close to saturation or oversaturated with respect to calcite and dolomite, and under saturation with respect to anhydrite and halite (Table 2).

The groundwater temperatures in the present study range from 28 to 43°C with an average of about 37°C (Table 1) and are typical for this arid region (Abdoulkader et al., 2013). On the other hand, studied waters may not be considered "hot or thermal", neither in sense of Pentecost (2005), nor in sense of Schoeller (1962).

As the cation-anion relation $(Ca+Mg)-(SO_4+HCO_3)$ shows an excellent correlation with electric conductivity in Fig. 3a, where only #12 (center of the Bara plain) and #13 (shallow dugwell in alluviums) outstand, this relation appears as relevant indicator of the degree of geochemical evolution of groundwater. Indeed, the $(Ca+Mg)-(SO_4+HCO_3)$ vs $(Na+K)-(Cl+NO_3)$ diagram (Fig. 3b) offers a graphical overview revealing a similar overall evolutionary trend for groundwater issued from both the alluvium and basaltic geological formations. The term evolutionary refers here to both water-rock interaction and mixing. This trend starts with a Na-Cl-HCO_3 water type in the Dadin area (#22) and most alluvium groundwater (#1, #2, #3, #4) (-5 to -4 on the horizontal axis). In this group, the excess of Na compared to Cl and depletion in Mg+Ca compared to HCO_3+SO_4 is explained by re-freshening through cation exchange, that typically

ACCEPTED MANUSCRIPT

occurs when freshwater with high Ca and HCO_3 flushes sediments that had been in prolongated contact with Na (e.g. Baudron et al., 2016). The geochemical trend ends with a Na-Cl-SO_4 water type in the most mineralized basalt groundwaters, namely #7 and #8 (16 to 19 on the horizontal axis), located in the junction between the Grand Bara and the Petit Bara plains (see below). The origin of these highly mineralized groundwaters will be discussed further in this paper. Samples from #10 and #16 (9 on the horizontal axis) are displayed in-between the intermediate water type and the most mineralized groundwaters, most problably revealing a mixing between them (see Fig. 3c). Finally, the correlation with the mean depth of the well screens and the aforementioned cation-anion relation, as showed by Fig. 3d, shows the vertical component of this geochemical trend inside both aquifers, although samples from boreholes of the central area (#7 and #8), as well as geochemically intermediate samples (boreholes #10 and #16), show a slightly different tendency.

4.1.2 Insights into water origin

To better understand the origin of the sampled waters, anions have been isolated in a ternary diagram (Fig. 4A). According to Fig. 3a, waters evolve from HCO_3 corner to Cl vertex following a linear trend, also depicted by shallow groundwater interacting with Stratoid basalts (Awaleh et al. 2016). In the same manner, most of previously studied samples coming from surrounding areas are here clustered, but two water samples which interact with evaporites (mainly gypsum; Aboubaker 2012, Aboubaker et al. 2013). Although these sulfate samples were collected by the authors in sedimentary formation westward of the Dikhil region, they show similar effects to those previously highlighted. For example, waters interacting with gypsum do not result in a Ca-SO_4 composition, but Na-SO_4 probably due to Ca-Na exchange with clays and/or mixing with Na-Cl waters followed by precipitation of calcium as $CaCO_3$. Finally, our high salinity samples

ACCEPTED MANUSCRIPT

deviate from such common path, and point towards a Na-Cl geothermal waters of meteoric origin as Abhe (Fig. 4A), which are compositionally very different from Na-HCO_3 geothermal waters from Main Ethiopian Rift (Pürschel et al. 2013; Rango et al. 2009). The Langelier-Ludwig diagram (Fig. 4B) is particularly adapted to shows evolutionary trend and mixing, in particular if Na-HCO_3 waters are involved in the processes as in this case (Boschetti 2011). However, the fluid origin information gained from ternary anion diagram could be confused due to the overlap of water-rock interaction processes which involve mainly cations (Giggenbach 1991). Indeed: i) the Na-HCO_3 towards Na-Cl evolutionary trend of the samples is more scattered in comparison to that depicted in Fig. 4A; ii) the fields of geothermal waters of meteoric origin (Abhe) and seawater-derived (Asal) are interdigitated; iii) differences between Na-SO_4 and Na-Cl is not resolved. To better discern between the cations variations related to high temperature effects, possibly inherited by geothermal waters, and low temperature effects, samples are plotted in the geothermal square plot (Fig. 5A). In this diagram is evident how most of our samples fall on a path which joins two hypothetical fluids (Fig. 5A) corresponding to the isochemical dissolution of Dahla basalt and to the fluid equilibration with rock at shallow temperatures (20-40°C, Giggenbach 1988; Fig. 5A). According to Giggenbach (1995), this low temperature shift of the samples might also involve K-uptake or Na-release from clays. Therefore local geothermal waters, if involved in fluid generation, changed their cationic proportions due water-rock interactions at more supergenic conditions.

Finally, fluid origin is tentatively inferred by B/Cl and Br/Cl ratios plot (Fig. 5B). In their previous study, Aboubaker et al. (2013) detected a Br/Cl molar ratio range from 0.0045 to 0.0086, excluding in this manner contribution from halite or other seawater evaporites. These ratios are higher than detected in our samples: 0.0020 ± 0.0005 (Table 2). This range includes that of local seawater (Br/Cl = 0.0017; Sanjuan et al. 1990). However, Fig. 5B shows clearly that

ACCEPTED MANUSCRIPT

most of the sampled waters mimic the wide B/Cl variations detected in other Afar fluids. In particular, our samples are within a ternary mixing which includes basalt (# 14), meteoric-derived geothermal waters (e.g. Abhe; Awaleh et al. 2015) and seawater-derived geothermal waters (e.g. Asal; Sanjuan et al. 1990). Two samples from Bara alluvium show the highest Br/Cl ratios (#13 = 0.0039; #18 = 0.0028; Table 2), which in combination with their B/Cl could be explained by interaction with an Afar evaporite, originated by seawater-derived geothermal fluid (Fig. 5B).

4.1.3 Origin of CO_2

One surprising feature is how bicarbonate severely decreases along the flow path (Fig. 4c): from 6 to 7 meq/l in the less mineralized groundwater sample of the Dadin area (#22) and of Petit Bara alluvium (#2 and 3) to 1 meq/l in the most evolved groundwater samples, located in the central area (#8). As well, $\log PCO_2$ is found to decrease from -1.7, typical of soils, down to -3.1, while pH increases from 7.26 to 8.38 (see Table 1). Atmospheric CO_2 and the subsequent enrichment in the soil layer is therefore a major source of HCO_3 in the aquifer system, although other subsurface sources of HCO_3 like the release of HCO_3 following water-rock interaction or a geothermal enriched CO_2 cannot be misconsidered (Awaleh et al. 2016 and reference therein). Geothermal waters in Djiboutian Afar and Main Ethiopian Rift have similar mantle-like $\delta^{13}C(CO_2)$ of approximatively -3.5 ‰ (e.g. Demlie et al., 2008, Alemayehu et al., 2011; Awaleh et al. 2016); however, the former have acid pH and no-HCO_3 in comparison to the alkaline high HCO_3 of the latter (Awaleh et al. 2016; D'Amore et al. 1998; Teklemariam and Beyene 2001). As illustrated by Fig. 6a, studied samples evolve from -18.5‰ vs PDB (at a HCO_3 value of 6.6 meq/l) which is quite close to the value of soil CO_2 (e.g. Cerling et al. 1991), to -12.7‰ vs PDB at 1.8 meq/l. The high HCO_3 – low $\delta^{13}C(CO_2)$ end-member could be due to the weathering in

ACCEPTED MANUSCRIPT

open system CO_2 condition (e.g. Clark 2015). Differently, taking into account the alkaline pH of the sampled waters and their saturation indexes (Table 1 and Table 2), the low HCO_3 - high $\delta^{13}C(CO_2)$ side could be originated by calcite equilibrium/oversaturation rather than deep CO_2 contributions.

4.1.4 Origin of nitrate

It is worth noting that all boreholes are used for drinking purpose, although for many of them, NO_3^- contents lie around the maximum permissible value prescribed by the World Health Organization standard set for drinking waters (50 ppm; WHO, 2011; see Table 2). The lowest values are found in Petit Bara and Dadin (Fig. 7a), while the highest values are found in Grand Bara (up to 250 mg/l in alluvium groundwaters from boreholes #13 and #18; up to 150 mg/l in basalt groundwaters from #11 and #12) and in the central area (up to 120 ppm in #7 and #8). It should be noted that people living in the Republic of Djibouti are mostly nomad, and hence have no agricultural tradition. Furthermore, the local nomads, who raise goats, cheeps, cows and camels, do not have a fixed settlement, hence not septic tanks. Therefore, in many cases, natural soil might contribute mainly for nitrate concentrations in the study area as observed in some semi-arid or arid regions over the world (Stadler et al., 2008; Walvoord et al., 2003). Exceptions concerned samples from boreholes like #13 and #18 whose nitrate content might feature anthropogenic forcing (Fig. 7a). To better constrain its origin we used the isotopic composition of nitrate ($\delta^{15}N–NO_3^-$ and $\delta^{18}O–NO_3^-$). As shown in Table 3 and illustrated by Fig. 7b, most values are located in a narrow range between 6.47 and 9.31 ‰ vs AIR for $\delta^{15}N–NO_3^-$ and 7.15 and 12.74 ‰ vs VSMOW for $\delta^{18}O–NO_3^-$ (Table 3). According to published N-isotope ranges

ACCEPTED MANUSCRIPT

(Kendall, 1998; Kendall et al., 2007; Aravena and Mayer, 2010), these groundwaters may all be affected by either sewage/manure and/or soil nitrogen. Taking into account the local oxygen isotope effect during nitrification (2/3 of O from H_2O between -4 and -1 from aquifer and +6‰ from evaporated rain, see next paragraph, and 1/3 from atmospheric $\delta^{18}O\text{-}O_2$ = +23.5‰; Kendall et al., 2007) and denitrification, the high nitrate concentration of borehole #18 (255 mg/l) could be derived from a denitrified manure source. However, because of the overlapped isotopic values of reduced nitrogen precursors (Fig. 7b) and the not well defined fractionation effects on oxygen during nitrification (Casciotti et al., 2011), nitrate isotopes can hardly differentiate different sources (Fenech et al., 2012). Anyway, considering the similar trend of #18 and #13 in Fig. 7a, the same sources could be hypothesized for the shallow borehole #13 (19m deep). Similarly, the dual isotopes ($\delta^{15}N\text{–}NO_3^-$ and $\delta^{18}O\text{–}NO_3^-$) are not suitable in differentiating closely related sources of nitrate contamination, such as sewage and manure, for Mouloud aquifer (boreholes #19 and #20) (Fig. 7b). These nitrate and chloride contents of the basalt aquifer in the studied area are very similar to the mean value revealed in the bordering Dalha basalt aquifer (Aboubaker, 2012; Fig. 7a). On the other hand, the $\delta^{15}N\text{–}NO_3^-$ and $\delta^{18}O\text{–}NO_3^-$ of boreholes #9, #11, #14, #17, and #22 indicate that the nitrate in those groundwaters is mainly derived from naturally occurring soil (Fig. 7b).

The #7 borehole, drilled in 2014 in the south of Wea valley, displays high nitrate content (119 mg/l) and appears as an outlier due to its high $\delta^{18}O\text{–}NO_3^-$ value of 16.8 ‰, that places it in the typical desert field trend as depicted by Jackson et al. (2015). Hydrogeochemical and isotopic findings further described in this paper evidenced that its mineralization was influenced by palaeowater of geothermal origin. Likely, the deep nitrogen signature of $\delta^{15}N$ = -5‰ (e.g. Li et al. 2016) was obliterated by paleoenvironmental factors related to former vegetation cover (e.g;

ACCEPTED MANUSCRIPT

Stadler et al., 2008) and/or accumulation of atmospheric nitrate in caliche and calcrete, which given their imprint for concomitant high NO_3-Cl contents and $\delta^{18}O–NO_3^-$ values to the recharging waters, as observed in several semi-arid and arid regions of the world (Fig. 7b; Al-Taani and Al-Qudah, 2013; Edmunds and Gaye, 1997; Jackson et al., 2015; Walvoord et al., 2003). As future perspective, and according to Dietzel et al. (2014) and Jackson et al. (2015), the analysis of perchlorate and ^{17}O in nitrate would be better clarify and trace the cross contamination between different nitrate sources.

4.1.5 Water isotope and recharge conditions

The oxygen $\delta^{18}O$ and hydrogen $\delta^{2}H$ stable isotopes are useful tracers for determining the origin of groundwater and are widely used in studying the natural water circulation and groundwater movement. One main task before interpreting such tracers is to set up a meteoric water line that will serve as a reference regarding fractionation and mixing processes. Since no systematic isotopic dataset concerning rainfall is available for Djibouti, most local studies choose the local meteoric water line (LMWL) from Addis Ababa station (e.g. Adam and Fontes, 1982; Aboubaker et al., 2013). Nonetheless, Addis Ababa is separated from the study area by more than 600 km of distance and is located almost 1800 m higher in altitude (2355 m a.s.l compared to around 600 m a.s.l). Furthermore, the study area is drier and hotter (about 150 $mm.y^{-1}$ and 34°C, respectively) than Addis Ababa (> 2500 $mm.y^{-1}$ and 16.5°C, respectively). Therefore, data from Addis Ababa might not provide realistic data for the study area. Local rainfall data from Djibouti is scarse (Adam and Fontes, 1982; Houmed-Gaba 2009) but provides interesting insights in accordance with a deuterium excess value of d = 2 (Fig. 8). This latter value coincides with that of the LMWL proposed by Fontes et al. (1979) and with a fractionation effect caused by secondary

ACCEPTED MANUSCRIPT

evaporation of the falling raindrops leading to a deuterium excess in rainfall, originated from both Atlantic monsoon ("pseudo-altitude effect"; Kebede, 2004) and from Indian monsoons (Pang et al., 2004). In the present study, despite the very little number of isotope measurements in Djibouti rainfall and to the high temporal variability of rainfall isotope composition in arid climate, we selected the aforementioned LMWL from Fontes et al. (1979), based on three rainfall samples, as the most probable orientative proxy of the isotopic composition of local precipitation, although it cannot be used as an absolute reference for evaporative effects.

As illustrated by Fig. 8, groundwater samples are mostly located along a line parallel to both the global meteoric water line (GMWL) and the LMWL, with a deuterium excess value of approximately 6. Therefore, no evaporation effect is evidenced, although sample from borehole #7 is located below this line and might reveal a slight fractionation process. Two samples from Fontes et al. (1980) are also located below this line, but it could simply be partly due to the difference between analytical laboratory techniques. Previous sections revealed the common geochemical evolution pattern of alluvium and basalt groundwaters. By difference, the $\delta^{2}H$ and $\delta^{18}O$ composition of groundwater (see Table 3 and Fig. 8) show that alluvium and basalt groundwater samples can be separated into two groups. The first cited have $\delta^{18}O$ values ranging from -1.9 to -1.1 ‰, i.e. in the range of wadi-recharged aquifers according to Fontes et al. (1979) and Awaleh et al. (2015) and in the range of modern precipitation for the area, according to Clark and Fritz (1997). Basalt groundwaters range between -3.9 and -2.6 ‰, rather close to Lake Abhe hot springs (Fontes et al., 1980; Awaleh et al., 2015). Two outsiders, alluvium groundwater from borehole #10 (northwestern Grand Bara) and basalt groundwater from borehole #22 (Dadin area), are located in the respective opposite categories. The $\delta^{2}H$ and $\delta^{18}O$ difference between alluvium and basalt groundwater can be explained by two hypotheses, or their combination: (i) recharge

ACCEPTED MANUSCRIPT

water is isotopically depleted in the highest basaltic outcrops (up to 1000 m a.s.l) compared to the plains (down to 600m a.s.l) because of altitude effects and (ii) recharge to the basalt groundwater occurred under a past climate, with cooler temperatures than present (e.g. Jirakova et al., 2011, Baudron et al., 2014). A $\delta^{18}O$ altitudinal gradients for Djibouti can be calculated based on the one proposed by Kebede et al. (2008) for Ethiopia: 0.1‰ per 100m. In such case, a 0.4‰ difference between alluvium and basalt groundwater would be found, much less than the mean difference between both (around 2.4‰) and rather in the range of variability inside one category. An altitude gradient value of 0.6‰ per 100m would be required to support such difference. Nonetheless, it would represent a very high value compared to global literature, while Levin (2008) considered the altitude effect to be mostly muted in Eastern Africa. Therefore, in addition to a possible slight altitude effect, the basalt groundwater is considered to be recharged under a past climate, in comparison to a recharge by more recent precipitation for the alluvium. Meaningful information to this respect is provided by time tracers in the next section.

4.1.6 Groundwater residence time

The only available tritium data for Djibouti precipitation are in the mid-eighties (Grand Bara area: 7.3 ± 0.7 TU; Dikhil area: 8.6 ± 1.3 TU and Mouloud area < 2.3 TU) (BGR, 1982). Coastal/low latitude tritium table of Clark and Fritz (1997) was therefore used to distinguish between modern and sub-modern (pre-bomb) waters. In the mid-seventies and early-eighties, the basalt groundwaters from #20 (Mouloud area), #16 (Grand Bara) and #12 (central Grand-Bara) boreholes displayed no measurable tritium (< 4T.U in Fontes et al., 1980 and < 2.2 T.U in BGR, 1982). By difference, alluvium groundwater from #3 (Petit Bara area) featured in 1975 up to 7 T.U. (Fontes et al., 1980) and therefore revealed a significant modern recharge component.

ACCEPTED MANUSCRIPT

Updated tritium data covering a wider spatial scale (11 samples) is brought by the present study. Similarly to previous campaigns by Fontes et al. (1980) and BGR (1982), no measurable tritium was found in any of the basalt groundwaters (<0.6 T.U), sampled in five boreholes from both the Mouloud and Grand Bara area. By comparison, tritium was detected in three of the six alluvium groundwater samples, issued from both the Petit Bara (#2 and #6 boreholes; 0.7 and 1.2 T.U, respectively) and Grand Bara areas (#13 borehole; 0.8 T.U). These results confirm an elder age for basalt groundwater than for the alluvium, where significant recharge from modern precipitation occurs.

In the early eighties, six groundwater samples were collected for radiocarbon and ^{13}C analysis by Fontes et al. (1980) and BGR (1982). They were collected from four basalt boreholes from the Mouloud, Grand Bara and central Grand Bara area and from one alluvium borehole from the Petit Bara area (Table 3). Since little detail was provided on the assumptions related to the correction of radiocarbon ages, they were recalculated in the present study. Calculating groundwater ages requires taking into account the initial composition of soil gas and correcting the measured activities with respect to water-rock interactions (e.g. Fontes, 1992; Baudron et al., 2013) if necessary. The progressive enrichment in $\delta^{13}C$ with decreasing $A^{14}C$ (Fig. 5a) appeared as an indicator of isotopic exchange with rock-matrix carbonate (e.g. Gillon et al., 2009). Therefore, the IAEA (Gonfiantini, 1972; Salem et al., 1980) age correction method was plebiscited to simpler methods like Tamers (Tamers, 1967). In fact, Table S1 (see supporting information) reveals unrelevant results for most data from other correction methods when using the criteria mentioned below. The $\delta^{13}C$ and $A^{14}C$ of the solid carbonates were set up to values of 0. Regarding the $\delta^{13}C$ of soil gas, Table 3 suggests an effect of both C3 and C4 plants, as supposed by Bocherens et al. (1996). Since no precise information was available on their respective location regarding recharge processes (e.g. basaltic outcrops, alluvium), a $\delta^{13}C(CO_2)$ value for

ACCEPTED MANUSCRIPT

soil gas of -21‰ vs PDB was set, as also proposed by Fontes et al. (1980) and close to the most depleted $\delta^{13}C(CO_2)$ calculated in groundwater (Table 3). On this basis, indicative rounded radiocarbon groundwater ages of 6250 years BP (before present, borehole #16 from the Grand Bara basalts), 2250 and 3100 years BP (boreholes #20 and #21 from the Mouloud area) and 10100 years (borehole #12 from the central Grand-Bara area) are obtained for basalt groundwater. By difference, alluvium groundwater (#3) age is 23 years BP (i.e., modern, sampling by Fontes, 1980) and 1050 years BP (sampling by BGR, 1982). The last value is probably impacted by intra-borehole mixing with older water, since this borehole features a long screen catching both alluvium and basalt and its geochemical and isotopic composition varies along time between both end-members (CERD, 2014). Based on the calculated radiocarbon groundwater ages, an important modern (post nuclear bomb tests) component of recharge is confirmed in the alluvium groundwater, while recharge is dated between the early and mi-Holocene in the basalt. These radiocarbon results only refer to a few discrete samples. Nonetheless, since $\delta^{13}C(CO_2)$ is linked to both decreasing HCO_3^- (Fig. 6b) - as an indicator of the geochemical evolution of groundwater - and $\delta^{18}O$ (Fig. 6c) - as an indicator of modern and old recharge - $\delta^{13}C$ might be used as a qualitative indicator of the evolution of groundwater age, thus generalizing the groundwater age pattern to the whole study area.

4.2 Insights into groundwater flow pattern

4.2.1 Overall groundwater flow pattern inside basalt groundwater

The #15 – #17 boreholes from the South of the Grand Bara area present comparable isotopic contents ($-3.7‰ \leq \delta^{18}O \leq -3.1‰$; $-24.8‰ \leq \delta^{2}H \leq -18.8‰$) to boreholes taping the Mouloud volcanic aquifer (#19 and #20). Besides, groundwater samples from boreholes #15 – #17 and #19

ACCEPTED MANUSCRIPT

– #20 have almost the same Na–Cl–Mg–SO_4 facies (Table 1) and are located in the same range of Ca+Mg-(SO_4+HCO_3) values (Fig. 3a). Therefore, the Grand Bara and Mouloud basalt aquifers are considered to be interconnected, forming one single volcanic aquifer (namely Grand Bara – Mouloud aquifer). Furthermore, according to potentiometric data (Fig. 2; Table S2 see supporting information), the moderately mineralized groundwaters from the Grand Bara – Mouloud area flows towards the North of the Grand Bara plain where the most mineralized groundwaters (#8, #12) are localized (Fig. 1). The high mineralization found in the central area (#8), i.e. the subterranean outlet of this endorheic plain, located at the geological threshold that separates Grand Bara and Petit Bara plains, is therefore most probably linked to the high residence time of groundwater and a subsequent higher level of water-rock interaction. A slight contribution of hydrothermal exchange with the host-rock also probably occurred for this sample (Fig. 8). Although they do not reach such high electric conductivity and show slightly different mineralization pattern, water sampled from the Abhe hot springs (Awaleh et al., 2015) are other examples of long-term water-rock interaction in the basalt formations, including a similar isotopic component of hydrothermal exchange with the host-rock (Awaleh et al., 2015).

4.2.2 From wadi-recharged alluvium to basalt aquifers

Continuity at the scale of the study area between the alluvium and basalt aquifers in terms of geochemical evolution and residence time of groundwater was shown in previous sections. Potentiometric levels bring complementary information regarding such connection. On the southwestern side of the Grand Bara plain (Mouloud), boreholes screened in an alluvial deltaic formation (#23, #24, #25) show higher potentiometric levels (by 20m, see Table S2) than deeper ones screened in the underlying basalt (#20, #26, #27). Such downward potentiometric relation is also observed in narrower wadi valleys like the one where is located #13, from the alluvium (#13)

ACCEPTED MANUSCRIPT

to the basalt (#14). There, the difference between the geochemical and isotopic signatures of both aquifer types is also clearly visible. As well, groundwater from Dadin basalts, located along a wadi-valley, features the isotopic and geochemical signature of modern wadi recharge water and therefore provides a confirmation of the connection between both compartments proposed by Aboubaker et al. (2013) at this location. This data demonstrates i) that recharge to alluvium is consistent in wadi valleys and in deltaic formation on the sides of the Grand Bara plain and ii) that it is transmitted downwards to the basaltic aquifers, probably through major faults.

Regarding the central Grand Bara plain, no direct interpretation can be made on the intensity of recharge processes to the alluvium and their transmission to basalt groundwater, since no data from the alluvium groundwater quality and hydrodynamics is available. Still, since the hydrology of Grand Bara plain is controlled by ephemeral floods caused by extreme rainfall events on a clayey surface, any significative contribution of recharge from the alluvium to the basalt groundwater would involve high evaporated stables isotopes of water. Nonetheless, as illustrated by #12, such feature is not found, while a high degree of geochemical evolution and thus long residence time is evidenced in basalt groundwater. Therefore, recharge from the alluvium in the central Grand Bara area is most probably insignificant, although it is consistent in the wadi valleys.

4.2.3 Refreshening by modern recharge at Petit Bara

The flowpath from Petit Bara plain to the Didjan Der valley, located northwestward and acting as its main outlet, is characterized by a continuous refreshening from 6.5 mS/cm (#7) to 2.8-2.9 mS/cm (#6 and #5), to around 1 mS/cm (#4, #3, #2) and below 1 mS/cm (#1), as shown in Table 1. Such process is confirmed by the $Ca+Mg-(SO_4+HCO_3)$ proxy of geochemical evolution (Fig. 9a) that decreases from values higher than 15 meq/l (#7) to slightly above 0 meq/l (#6 and #5)

ACCEPTED MANUSCRIPT

and finally around -5 meq/l (#4, #3, #2, #1). A similar tendency of decreasing evolution is observed with isotopic tracers $\delta^{18}H$ (Fig. 9b) and $\delta^{13}C$(DIC) (Fig. 9c) whose compositions evolve from the isotopic signature of basalt groundwater (-3.7 ‰ vs V-SMOW and -12.7 ‰ vs PDB, respectively) to the one of freshly recharged alluvium groundwater (-1.1 vs V-SMOW and -18.3 ‰ vs PDB, respectively). As a consequence, recharge from the Didjan Der valley is consistent and induces a refreshening process of groundwater flowing out from the Petit Bara plain. This feature is an additional evidence of the consistent recharge occurring in the riverbed of wadi rivers as well as it provides insightful information on groundwater flowpath in the Petit Bara area. Regarding the salinity increase of the #6 groundwater over time (CERD, 2014), it should be due to an overexploitation that may bring back #7 or #8 highly mineralized waters by upcoming (Lorenzen et al., 2011), as proposed by Fig. 3d.

4.2.4 Strontium isotope ratio: complementary insight on groundwater origin

The $^{87}Sr/^{86}Sr$ ratio measured in water reflects the distinct isotopic composition of the interacting rocks and can furnish information on groundwater flowpaths and hydrodynamics (Drever, 1997; Barbieri et al., 2005). The $^{87}Sr/^{86}Sr$ isotopic ratios of the investigated groundwater samples range from 0.70556 to 0.70694 (Table 3). These data are compared with the $^{87}Sr/^{86}Sr$ values of local lithotypes available in the literature in order to define the nature of the interacting rocks. The reported Sr isotopic values of basalt samples from the Republic of Djibouti show considerable variation from 0.70350 to 0.70664, with the lower value corresponding to the most recent Afar mantle plume (Vidal et al., 1991; Barrat et al., 1993; Deniel et al., 1994; Rogers, 2006). Barrat et al. (1993) reported that the pre-Dalha basalts, which are often weathered, show a large variation in $^{87}Sr/^{86}Sr$ ratios from 0.7037 to 0.7067. On the other hand, for the non weathered basalts of the

ACCEPTED MANUSCRIPT

Dalha series (8.3-4.3 Ma), the mean Sr isotopic composition is quite uniform: 0.70411 ± 0.00047 (Barrat et al., 1993; Deniel et al., 1994; Vidal et al., 1991). Almost all the investigated groundwater lies outside the non weathered Dalha basalt range, suggesting contributions from more radiogenic rocks along the groundwater flow path, for example: i) lacustrine sediments; ii) weathered Dalha basalt or more radiogenic rocks (e.g. rhyolites). Some evidences support this latter hypothesis. For examples, drilling logs revealed that most of the Dalha basalts in the study area are weathered. Moreover, the highest $^{87}Sr/^{86}Sr$ values of the water samples were revealed in the southern side of the Bara plain (boreholes #22, #13, #14, #11). It is reasonable to assume that some amounts of the radiogenic strontium in the local weathered basalt or alluvium come from the older Mablas rhyolite (up to 0.722; Deniel et al., 1994).

Most of the $^{87}Sr/^{86}Sr$ of dissolved Sr in Djibouti (SanJuan et al., 1990; Dekov et al., 2014; Awaleh et al., 2015; Awaleh et al., 2016) pertain to geothermal waters issuing from Stratoid and Asal rift basalts (which have not so different strontium isotope ratio from Dahla basalt, Faure 2001; Fig. 10a) which have a relatively low $^{87}Sr/^{86}Sr$, testifying a full or partial equilibration with the source rock (Fig. 9a; Awaleh et al., 2015; Sanjuan et al., 1990; unpublished data). Exceptions include shallow groundwater (Awaleh et al., 2016) and waters interacting with alluvial deposits. As an example of this latter case, Oued-Kalou springs near to Lake Asal area show similar composition to the waters from this study (Fig. 10a; Sanjuan et al. 1990). Moreover, the statistically significative linear relationship between sulfate and strontium of the Bara groundwater testify the big effect of alluvial component on the Sr isotope ratio (Fig. 10b). Therefore, the high $^{87}Sr/^{86}Sr$ ratios observed for the investigated groundwater from volcanic aquifers might be related to different contributions: not only Dalha basalt and its alteration products in this study area, but also the recharge of the volcanic aquifers through major faults by

ACCEPTED MANUSCRIPT

waters interacting with alluvial deposits which mediate the contribution of surrounding formations.

5. Conclusion

This integrated study aimed at revealing the recharge conditions, groundwater age distribution, origin of contaminants and groundwater flow pattern inside the complex volcanic aquifer system of Bara (Djibouti). To this end, an integrated hydrodynamic, geochemical and isotopic approach was set up. Geochemistry showed an evolutionary trend from alluvium aquifers located in wadi-valleys and deltaic formations bordering the main sedimentary basins (Petit Bara and Grand Bara), with low salinity groundwater and Na-Cl-HCO_3 water type, to a more saline and intermediate water type in most basalt groundwaters (Grand Bara and Mouloud area) and finally to a Na-Cl-SO_4 water type in the most mineralized groundwaters located at the border between Grand Bara and Petit Bara. Elementary and isotopic nitrate evidenced anthropogenic and geogenic origins of nitrate. Stable isotopes of water revealed modern recharge in the alluvium through infiltration of precipitation in wadi aquifers and revealed significantly depleted values in the second. No evaporation effects were evidenced, since most groundwater samples plotted on a $\delta^{18}O$ vs $\delta^{2}H$ line parallel to both global and local precipitation lines. Modern radiocarbon and tritium were evidenced in the alluvium groundwaters, while recalculated radiocarbon ages located recharge of the basalt groundwaters in the early to mid-Holocene. These features revealed a common evolutionary pattern, with a significant recharge from the alluvium, transmitted downward to the basalt aquifer through major faults in the wadi valleys or through the sediments of the alluvial fans, followed by mixing with ancient Na-Cl water. This latter endmember with depleted content of ^{2}H and ^{18}O isotopes could be a deep and old geothermal water from the

ACCEPTED MANUSCRIPT

Stratoid basalts, then cooled and evolved after interaction with Dalha basalts. This study also revealed strategic characteristic of the groundwater flow pattern. Two major basaltic aquifer compartments, the Grand Bara and Mouloud aquifers, were found to form one single aquifer flowing northeastward below the Grand Bara endorheic plain. Highly mineralized groundwater flowing out from the Petit Bara basin was found to be rapidly diluted by modern recharge in the alluvium of the Didjan Der valley. In addition to providing significant insights for a groundwater management of the Bara area, this study will also serve as a valuable base for other integrated hydrodynamic, geochemical and isotopic studies of volcanic aquifers in arid areas.

Acknowledgements

This research work was financially supported by the United Nation Development Program (UNDP), the Centre d'Etudes et de Recherche de Djibouti (CERD), and the International Foundation for science, Stockholm, Sweden, through a grant N^{o} W/5800-1. We would like to thank Mr Aden Atteyeh for fruitful discussion and Mr Samaleh Ahmed Idriss and Abdi Abdillahi Djibril for their assistance in the field works. We would also like to thank two anonymous reviewers for their constructive comments that improved the manuscript.

Table and Figure captions

Table 1. Sampling locations, T, depth, pH, EC, TDS and hydrochemical types of the sampled waters.

Table 2. Hydrochemical characteristics (in mg/l) of water samples in the study area and saturation index (SI) of selected minerals.

Table 3. Isotope data of Bara groundwaters from this study and literature.

ACCEPTED MANUSCRIPT

Figure 1. Geological map of the study area (EAR = East African Rift).

Figure 2. Geological cross-sections in Petit Bara (a), Mouloud-Grand Bara (b) and Mouloud (c) areas.

Figure 3. Variations of EC (a), (Na+K)-(Cl+NO_3) (b), HCO_3 (c) and half depth of the screen (d) versus the (Ca+Mg)-(HCO_3+SO_4) indicator of geochemical evolution.

Figure 4. Anions ternary diagram, mg/l basis (a) and Langelier-Ludwig square plot, meq/l basis (b). Volcanic, geothermal and peripheral/shallow fields are from Giggenbach (1988); dotted field depicts samples collected by Aboubaker (2012) and Aboubaker et al (2013); fields with different hatches distinguish meteoric-derived (Abhe; Awaleh et al. 2015) and seawater-derived (Sakalol, Asal; Awaleh et al. 2016) geothermal waters, respectively.

Figure 5. (a) Geothermal square plot (Giggebach 1988): dashed lines describe the evolution of the waters from isochemical dissolution of Dahla basalt (Mohr and Zanettin 1988) towards low temperature equilibrium with average crust (full equilibrium line, numbers are temperature in Celsius degrees; Giggebanch 1988). Dotted field as in Fig.4. (b) B/Cl vs. Br/Cl diagram. Agriculture drainage, sewage and seawater evaporites fields are drawn according to Vengosh (2014). Afar Hydrothermal waters describes waters of meteoric origin, whereas mean ± standared deviation crosses depict geothermal or regional waters from Afar with variable seawater contributions (Awaleh et al. 2016, Lowenstern et al. 1999, Sanjuan et al. 1990; UNDP 1973). Afar evaporites (Binega 2006, Martini 1977), Basalts (Awaleh et al. 2016) and Main Ethiopian Rift (M.E.R.; Gianelli and Teklemariam 1993, Pittalis et al. 2016) fields are also shown for comparison.

ACCEPTED MANUSCRIPT

Figure 6. Variations of HCO_3 (a), $A^{14}C$ (b) and $\delta^{18}O$ (c) versus $\delta^{13}C\text{-}CO_2$. Samples with a circle are taken from the literature (Fontes et al., 1979; BGR, 1982). In (b), rounded mean apparent ages calculated with the IAEA correction method.

Figure 7. $\delta^{15}N\text{-}NO_3$ versus $\delta^{18}O\text{-}NO_3$ diagram (a) of the groundwaters from the study area, in comparison with nitrates derived from typical: i) N sources after nitrification by local waters (Aravena and Mayer 2010; Kendall 1998; Kendall et al., 2007); ii) desert nitrates (Jackson et al., 2015). Nitrate vs. chloride plot (b).

Figure 8. $\delta^{18}O$ versus $\delta^{2}H$ diagram of the groundwaters from the study area showing the global meteoric water line (GMWL after Craig, 1961) and local meteoric water line (LMWL after Fontes et al. 1979). d accounts for the deuterium excess. Samples with a circle are taken from the literature (Fontes et al., 1979; BGR, 1982; Aboubaker et al., 2013).

Figure 9. Variations of $Ca+Mg\text{-}(HCO_3+SO_4)$ (a), $\delta^{18}O$ (b) and $\delta^{13}C\text{-}CO_2$ (c) along the flowpath from Petit Bara plain to Didjan Der valley. Samples with a circle are taken from the literature (Fontes et al., 1979; BGR, 1982).

Figure 10. Relationship between $^{87}Sr/^{86}Sr$ and 1/Sr (a). Curves depict the best fits of hot springs issuing from active geothermal systems from Asal rift ("marine" curve; data from Sanjuan et al., 1990) and Stratoid basalts ("meteoric" curve; Abhe waters: Awaleh et al., 2015; Awaleh et al. 2016). It is noteworthy that values detected in the Main Ethiopian Rift (Rango et al. 2010) fall on the high 1/Sr - high $^{87}Sr/^{86}Sr$ range of the "meteoric curve". Open circles: hot springs from alluvial deposits, SW of Lake Asal (Oued-Kalou; Sanjuan et al., 1990). Strontium isotope ratios of Quaternary basalts and Afar rift are from Faure (2001) and Rooney et al. (2012). Strontium vs. sulfate plot (b), with an additional sample from Oued-Kalou (Bosch et al., 1977).

ACCEPTED MANUSCRIPT

References

Aboubaker M. 2012. *Caractérisation d'un système aquifère volcanique par approche couplée hydrogéochimique et modélisation numérique. Exemple de l'aquifère des basaltes de Dalha, sud-ouest de la République de Djibouti*. PhD thesis, University of Poitiers, France.

Aboubaker M, Jalludin M, Razack M. 2013. Hydrochemistry of a complex volcano-sedimentary aquifer using major ions and environmental isotopes data: Dalha basalts aquifer, southwest of Republic of Djibouti. Environmental Earth Sciences 70**,** 3335-3349. DOI: 10.1007/s12665-013-2398-8

Adam A, Fontes JC. 1982. Etude hydrogéologique et hydrochimique de la partie septentrionale de la République de Dibouti. Djibouti. 105 pp.

Alemayehu T, Leis A, Eisenhauer A, Dietzel M. 2011. Multi-proxy approach ($^{2}H/H$, $^{18}O/^{16}O$, $^{13}C/^{12}C$ and $^{87}Sr/^{86}Sr$) for the evolution of carbonate-rich groundwater in basalt dominated aquifer of Axum area, northern Ethiopia. Chemie der Erde – Geochemistry 71, 177–187. DOI: 10.1016/j.chemer.2011.02.007

Al-Taani AA, Al-Qudah KA. 2013. Investigation of desert subsoil nitrate in Northeastern Badia of Jordan. Science of the Total Environment 442, 111–115. DOI: 10.1016/j.scitotenv.2012.10.018

Aravena R, Mayer B. 2010. Isotopes and Processes in the Nitrogen and Sulfur Cycles. In: Aelion CM, Aravena R, Hunkeler D, Höhener P (eds.), *Environmental Isotopes in Biodegradation and Bioremediation*. Chapter 7, CRC Press, 203–246.

ACCEPTED MANUSCRIPT

Arthaud F, Jalludin M. 1993. *Cartographie des fractures d'un réservoir hydrogéologique en milieu volcanique à partir de données HRV de SPOT contrôlées sur le terrain* (basaltes miocènes de Djibouti). Télédétection et cartographie. Éd. AUPELF-UREF. Les Presses de l'Université du Québec. 83-94.

Audin L, Quidelleur X, Coulié E, Courtillot V, Gilder S, Manighetti I, Kidane T. 2004. Palaeomagnetism and K-Ar and 40Ar/39Ar ages in the Ali Sabieh area (Republic of Djibouti and Ethiopia): constraints on the mechanism of Aden ridge propagation into southeastern Afar during the last 10 Myr. Geophysical Journal International 158, 327-345. DOI: 10.1111/j.1365-246X.2004.02286.x

Awaleh MO, Hoch FB, Boschetti T, Soubaneh YD, Egueh NM, Elmi SA, Jalludin M, Khaireh MA. 2015. The geothermal resources of the Republic of Djibouti – II: geochemical study of the Lake Abhe geothermal field. Journal of Geochemical Exploration 159, 129–147. DOI: 10.1016/j.gexplo.2015.08.011

Awaleh MO, Boschetti T, Soubaneh YD, Baudron P, Kawalieh AD, Dabar OA, Ahmed MM, Ahmed SI, Daoud MA, Egueh NM, Jalludin M (2016) Geochemical study of the Sakalol – Harralol geothermal field (Republic of Djibouti): evidences of a low enthalpy aquifer between Manda-Inakir and Asal rift settings. Journal of Volcanology and Geothermal Research (in press) DOI: 10.1016/j.jvolgeores.2016.11.008

ACCEPTED MANUSCRIPT

Barberi F, Ferrara G, Santacroce R, Varet J. 1975. Structural evolution of the Afar triple junction. In: Pilger A, Rosler A (eds.), *Afar Depression of Ethiopia*. Inter-Union Commission on Geodynamics, Scientific Report 14, E. Schweizerbart'sche Verlagsbuchhandlung (Nägele u Obermiller), Stuttgart, pp. 38–54.

Barbieri M, Boschetti T, Petitta M, Tallini M. 2005. Stable Isotope (^{2}H, ^{18}O and $^{87}Sr/^{86}Sr$) and hydro-geochemistry monitoring for groundwater hydrodynamics analysis in a karst aquifer (Gran Sasso, Central Italy). Applied Geochemistry 20, 2063-2081. DOI: 10.1016/j.apgeochem.2005.07.008

Barrat JA, Jahn BM, Fourcade S, Joron JL. 1993. Magma genesis in an ongoing rifting zone: the Tadjoura Gulf (Afar area). Geochimica et Cosmochimica Acta 57, 2291–2302. DOI: 10.1016/0016-7037(93)90570-M

Baudron P, Barbecot F, Gillon M, García-Aróstegui JL, Travi Y, Leduc C, Gomariz Castillo F, Martinez-Vicente D. 2013. Assessing Groundwater Residence Time in a Highly Anthropized Unconfined Aquifer Using Bomb Peak 14C and Reconstructed Irrigation Water 3H. Radiocarbon 55; 993-1006. DOI: 10.2458/azu_js_rc.55.16396

Baudron P, Barbecot F, Aróstegui JLG, Leduc C, Travi Y, Martinez-Vicente D. 2014. Impacts of human activities on recharge in a multilayered semiarid aquifer (Campo de Cartagena, SE Spain). Hydrological Processes 28, 2223–2236. DOI: 10.1002/hyp.9771

ACCEPTED MANUSCRIPT

Baudron P, Sprenger C, Lorenzen G, Ronghang M. 2016. Hydrogeochemical and isotopic insights into mineralization processes and groundwater recharge from an intermittent monsoon channel to an overexploited aquifer in eastern Haryana (India). Environmental Earth Sciences 75, 1–11. Doi:10.1007/s12665-015-4911-8

BGR 1982. Inventaire et mise en valeur des ressources en eau de la République de Djibouti. Coopération Hydrogéologique Allemande. BGR (Bundesanstalt für Geowissenschaften und Rohstoffe). Volume IV – Inventaire des points d'eau. Projet N78.2233.1 ; BGR92705. Hannover, Germany, June 1982. Republic of Djibouti. 157p.

Binega Y. 2006. Chemical analysis of the Assale (Ethiopia) rock salt deposit. Bulletin of the Chemical Society of Ethiopia 20, 319-324.

Bocherens H, Koch PL, Mariotti A, Geraads D, Jaeger JJ. 1996. Isotopic biogeochemistry (^{13}C, ^{18}O) of mammalian enamel from African Pleistocene hominid sites. Palaios 11, 306–318. DOI: 10.2307/3515241

Bosch B, Deschamps J, Leleu M, Lopoukhine M, Marcé A, Vilbert C. 1977. The geothermal zone of Lake Assal (F.T.A.I.), Geochemical and experimental studies. Geothermics 5, 166-175. DOI: 10.1016/0375-6505(77)90017-7

Boschetti T. 2011. Application of Brine Differentiation and Langelier-Ludwig plots to fresh-to-brine waters from sedimentary basins: diagnostic potentials and limits. Journal of Geochemical Exploration 108, 126-130. DOI: 10.1016/j.gexplo.2010.12.002

ACCEPTED MANUSCRIPT

Casciotti KL, Buchwald C, Santoro AE, Frame C. 2011. Assessment of nitrogen and oxygen isotopic fractionation during nitrification and its expression in the marine environment. Methods Enzymol 486, 253-280. DOI: 10.1016/S0076-6879(11)86011-8

CERD 2014. Etudes géochimiques, géophysiques et hydrogéologiques des forages de Petit Bara, Grand Bara et Mouloud-Dadin. Institut des Sciences de la Terre. Centre d'Etudes et de Recherche de Djibouti (CERD). Djibouti, Republic of Djibouti, Octobre 2014. 60p.

Cerling TE, Solomon DK, Quade JAY, Bowman JR. 1991. On the isotopic composition of carbon in soil carbon dioxide. Geochimica et Cosmochimica Acta 55, 3403-3405. DOI: doi:10.1016/0016-7037(91)90498-T

Clark ID. 2015. *Groundwater Geochemistry and Isotopes*. CRC Press.

Clark ID, Fritz P. 1997. *Environmental Isotopes in Hydrogeology.* CRC Press.

Craig H. 1961. Standards for reporting concentrations of deuterium and oxygen-18 in natural waters. Science 133, 1702–1703. DOI: 10.1126/science.133.3467.1833

D'Amore F, Giusti D, Abdallah A. 1998. Geochemistry of the High-salinity geothermal field of Asal, Republic of Djibouti, Africa. Geothermics 27, 197–210. DOI: 10.1016/S0375-6505(97)10009-8

ACCEPTED MANUSCRIPT

Daoud MA, Le Gall B, Maury RC, Rolet J, Huchon P, Guillou H. 2011. Young rift kinematics in the Tadjoura rift, western Gulf of Aden, Republic of Djibouti. Tectonics 30, 1 – 20. DOI: 10.1029/2009TC002614

Demlie M, Wohnlich S, Ayenew T. 2008. Major ion hydrochemistry and environmental isotope signatures as a tool in assessing groundwater occurrence and its dynamics in a fractured volcanic aquifer system located within a heavily urbanized catchment, central Ethiopia. Journal of Hydrology 353, 175–188. DOI: 10.1016/j.jhydrol.2008.02.009

Deniel C, Vidal P, Coulon C, Vellutini .J, Piguet P. 1994. Temporal evolution of mantle sources during continental rifting: the volcanism of Djibouti (Afar). Journal of Geophysical Research 99, 2853-286. DOI: 10.1029/93JB02576

Dekov V.M., Egueh N.M., Kamenov G.D., Bayon G., Lalonde S.V., Schmidt M., Liebetrau V., Munnik F., Fouquet Y., Tanimizu M., Awaleh M.O., Farah I.G., Le Gall B. 2014. Hydrothermal carbonate chimneys from a continental rift (Afar Rift): mineralogy, geochemistry and mode of formation. Chemical Geology 387, 87–100. DOI: 10.1016/j.chemgeo.2014.08.019

Dietzel M., Leis A, Abdalla R, Savarino J, Morin S, Böttcher ME, Köhler S. 2014. ^{17}O excess traces atmospheric nitrate in paleo-groundwater of the Saharan desert. Biogeosciences 11, 3149–3161. DOI: 10.5194/bg-11-3149-2014

Drever JI. 1997. The Geochemistry of Natural water. Prentice Hall.

ACCEPTED MANUSCRIPT

Edmunds WM, Gaye CB. 1997. Naturally high nitrate concentrations in groundwaters from the Sahel. Journal of Environmental Quality 26, 1231–1239. DOI: 10.2134/jeq1997.00472425002600050006x

Faure G. 2001. Origin of Igneous Rocks: The Isotopic Evidence. Springer-Verlag Berlin Heidelberg GmbH.

Fenech C, Rock L, Nolan K, Tobin J, Morrissey A. 2012. The potential for a suite of isotope and chemical markers to differentiate sources of nitrate contamination: a review. Water Research 46, 2023–2041. DOI: 10.1016/j.watres.2012.01.044

Fontes JC, Florkowski T, Pouchan P, Zuppi GM. 1979. Preliminary isotopic study of Lake Asal system (Republic of Djibouti). In: Mortimer C (ed), *Application of nuclear techniques to the study of lake dynamics*. Vienna, Aug. 20-Sept. 2, 163-174.

Fontes JC, Pouchan P, Saliege JF, Zuppi GM. 1980. Environmental isotope study of groundwater systems in the Republic of Djibouti. In: *Arid-zone Hydrology: Investigations with Isotope Techniques*, 237-262, IAEA, Vienna.

Fontes JC. 1992. Chemical and isotopic constrainsts on ^{14}C dating of groundwater. In: Taylor ED, Long A, Kra RS (eds), *Radiocarbon after four decades*. Springer-Verlag: New York; 242–261.

Gadalia A. 1980. *Les Rhyolites du stade initial de l'ouverture d'un rift : Exemple des Rhyolites Miocène de l'Afar*. PhD thesis, University of Orsay, Paris, France.

ACCEPTED MANUSCRIPT

Gasse F, Varet J, Mazet G, Recroix F, Ruegg JC. 1986. Carte géologique de la République de Djibouti à 1:100000, Ali Sabieh, notice explicative, ISERST, Ministère français de la Coopération, Paris

Gianelli G, Teklemariam M. 1993. Water-rock interaction processes in the Aluto-Langano geothermal field (Ethiopia). Journal of Volcanology and Geothermal Research 56, 429-445.

Giggenbach W.F. 1988. Geothermal solute equilibria Derivation of Na–K–Mg–Ca geoindicators. Geochimica et Cosmochimica Acta 52, 2749–2765. doi:10.1016/0016-7037(88)90143-3

Giggenbach W.F. 1991. Chemical techniques in geothermal exploration. In: Applications of Geochemistry in Geothermal Reservoir Development, (ed. D'Amore F.), pp. 119-142, UNITAR/UNDP publication, Rome.

Giggenbach W.F. 1995. Exploration of a "Difficult" Geothermal System, Paraso, Vella Lavella, Solomon Islands. Proceedings of the World Geothermal Congress, Vol. 2, 995-1000.

Gillon M, Barbecot F, Gibert E, Corcho Alvarado JA, Marlin C, Massault M. 2009. Open to closed system transition traced through the TDIC isotopic signature at the aquifer recharge stage, implications for groundwater 14C dating. Geochimica et Cosmochimica Acta 73, 6488–6501. DOI: 10.1016/j.gca.2009.07.032

Gonfiantini R. 1972. Notes on isotope hydrology. Internal Report, IAEA, Vienna

ACCEPTED MANUSCRIPT

Houssein I, Jalludin M. 1996. The salinity of Djibouti's aquifer. Journal of African Earth Sciences 22, 409–414. DOI: 10.1016/0899-5362(96)00024-3

Houmed-Gaba A. 2009. *Hydrogéologie des milieux volcaniques sous climat aride : caractérisation sur site expérimental et modélisation numérique de l'aquifère basaltique de Djibouti (Corne de l'Afrique)*. PhD Thesis, University of Poitiers, France.

IAH (International Association of Hydrogeologists) 1979. Map of mineral and thermal water of Europe. Scale 1:500.000. International Association of Hydrogeologists. UK.

Jackson WA, Böhlke JK, Andraski BJ, Fahlquist L, Bexfield L, Eckardt FD, Gates JB, Davila AF, McKay CP, Rao B, Sevanthi R, Rajagopalan S, Estrada N, Sturchio NC, Hatzinger PB, Anderson TA, Orris G, Betancourt J, Stonestrom D, Latorre C, Li Y, Harvey GJ. 2015. Global patterns and environmental controls of perchlorate and nitrate co-occurrence in arid and semi-arid environments. Geochimica et Cosmochimica Acta 164, 502-522. DOI: 10.1016/j.gca.2015.05.016

Jalludin M, Razack M. 1994. Analysis of pumping tests in fractured basalts with regards to tectonics, lvydrofhermalisms and weathering, Republic of Djibouti. Journal of Hydrology 155, 237-250. DOI: 10.1016/0022-1694(94)90167-8

ACCEPTED MANUSCRIPT

Jalludin M, Razack M. 2004. Assessment of hydraulic properties of sedimentary and volcanic aquifer systems under arid conditions in the Republic of Djibouti (Horn of Africa). Hydrogeology Journal 12, 159–170. DOI 10.1007/s10040-003-0312-2

Jimenez-Martinez J, Garcia-Arostegui JL, Hunink J, Contreras S, Baudron P, Candela L. 2016. The role of groundwater in highly human-modified hydrosystems: A review of impacts and mitigation options in the Campo de Cartagena-Mar Menor coastal plain (SE Spain). Environmental Reviews 24(4), 377-392. DOI 10.1139/er-2015-0089

Jirakova H, Huneau F, Celle-Jeanton H, Hrkal Z, Le Coustumer P. 2011. Insights into palaeorecharge conditions for European deep aquifers. Hydrogeology Journal 19, 1545–1562. DOI: 10.1007/s10040-011-0765-7

Kebede S. 2004. *Approches isotopique et geochimique pour l'étude des eaux souterraines et des lacs: Exemples du haut bassin du Nil Bleu et du rift Ethiopien* [*Environmental isotopes and geochemistry in groundwater and lake hydrology: cases from the Blue Nile basin, main Ethiopian rift and Afar, Ethiopia*], PhD thesis, University of Avignon, France.

Kebede S, Yves T, Asrat A, Alemayehu T, Ayenew T, Tessema Z. 2008. Groundwater origin and flow along selected transects in Ethiopian Rift volcanic aquifers. Hydrogeology Journal 16, 55–73. DOI: 10.1007/s10040-007-0210-0

ACCEPTED MANUSCRIPT

Kendall C. 1998. Tracing nitrogen sources and cycling in catchments. In: Kendall, C., McDonnell, J.J. (Eds.), *Isotope Tracers in Catchment Hydrology*. Elsevier Science B.V: Amsterdam; 519-576.

Kendall C., Elliott EM, Wankel SD. 2007. Tracing anthropogenic inputs of nitrogen to ecosystems. In: Michener R.H. and Lajtha K. (eds.), *Stable Isotopes in Ecology and Environmental Science*, 2nd edn., Ch. 12, Oxford Blackwell, 375–449.

Kharaka YK, Hanor JS. 2014. Deep Fluids in Sedimentary Basins. In: Holland HD & Turekian KK (eds) *Treatise on Geochemistry*, Second Edition, Elsevier: Oxford; 7, 472-515.

Le Gall B, Daoud MA, Maury RC, Rolet J, Guillou H, Sue C. 2010. Magma-driven antiform structures in the Afar rift: the Ali Sabieh range, Djibouti. Journal of Structural Geology 32, 843–854. DOI:10.1016/j.jsg.2010.06.007

Levin NA. 2008. *Isotopic Records of Plio-Pleistocene Climate and Environments in Eastern Africa*. PhD Thesis. University of Utah.

Li Y, Marty B, Shcheka S, Zimmermann L, Keppler H. 2016. Nitrogen isotope fractionation during terrestrial core-mantle separation. Geochemical Perspectives Letters 2, 138-147.

Lorenzen G, Sprenger C, Baudron P, Gupta D, Pekdeger A. 2011. Origin and dynamics of groundwater salinity in the alluvial plains of western Delhi and adjacent territories of Haryana State, India. Hydrological Processes 26, 2333-2345. DOI: 10.1002/hyp.8311

ACCEPTED MANUSCRIPT

Lowenstern J.B, Janik CJ, Fournier RO, Tesfai T, Duffield WA, Clynne MA, Smith JG, Woldegiorgis L, Weldemariam K, Kahsai G. 1999. A geochemical reconnaissance of the Alid volcanic center and geothermal system, Danakil depression, Eritrea. Geothermics 28, 161-187. DOI: 10.1016/S0375-6505(99)00002-4

Martini M. 1977. Le sorgenti termali del piano del sale (Etiopia). Rendiconti Società Italiana di Mineralogia e Petrologia 33, 773-780.

Mlynarski M, Zlotnicki J. 2001. Fluid circulation in the active emerged Asal rift (east Africa, Djibouti) inferred from self-potential and telluric–telluric prospecting. Tectonophysics 339, 455–472. DOI: 10.1016/S0040-1951(01)00127-5

Mohr P, Zanettin B. 1988. The Ethiopian Flood Basalt Province. In: J. D. Macdougall (ed.) Continental Flood Basalts, Volume 3 of the series Petrology and Structural Geology, Springer Netherlands, pp. 63-110. DOI: 10.1007/978-94-015-7805-9_3

Pang H, He Y, Zhang Z, Lu A, Gu J. 2004. The origin of summer monsoon rainfall at New Delhi by deuterium excess. Hydrology and Earth System Sciences 8, 115-118. DOI: 10.5194/hess-8-115-2004

Parkhurst D.L., Appelo C.A.J., 2015. Description of Input and Examples for PHREEQC Version 3--A Computer Program for Speciation, Batch-Reaction, One-Dimensional Transport, and Inverse Geochemical Calculations. (http://wwwbrr.cr.usgs.gov/projects/GWC_coupled/phreeqci/)

ACCEPTED MANUSCRIPT

Pentecost, A., 2005. Hot springs, thermal springs and warm springs. What's the difference? Geology Today, 21: 222–224.

Pittalis D., Petrella E., Bucci A., Naclerio G., Campari A., Sordella S., Celico F., Zanini A., Boschetti T., Toscani L. 2016. Multidisciplinary investigations for a safe drinking water supply of poor villages, Southern Ethiopia. AQUA 2015: Back to the Future! 42 International Congress of International Association of Hydrogeologists, Volume 39, suppl. 1

Pürschel M., Gloaguen R., Stadler S. 2013. Geothermal activities in the Main Ethiopian Rift: Hydrogeochemical characterization of geothermal waters and geothermometry applications (Dofan-Fantale, Gergede-Sodere, Aluto-Langano). Geothermics 47, 1-12. DOI: 10.1016/j.geothermics.2013.01.001

Rango T., Bianchini G., Beccaluva L., Ayenew T., Colombani N. 2009. Hydrogeochemical study in the Main Ethiopian Rift: New insights to the source and enrichment mechanism of fluoride. Environmental Geology 58, 109-118. DOI: 10.1007/s00254-008-1498-3

Rango T, Petrini R, Stenni B, Bianchini G, Slejko F, Beccaluva L, Ayenew T. 2010. The dynamics of central Main Ethiopian Rift waters: Evidence from δD, $\delta^{18}O$ and $^{87}Sr/^{86}Sr$ ratios. Applied Geochemistry 25, 1860-1871. DOI: 10.1016/j.apgeochem.2010.10.001

Rogers NW. 2006. Basaltic magmatism and the geodynamics of the East African Rift System. In: Yirgu G, Ebinger CJ & Maguire PKH (eds.), *The Afar Volcanic Province within the East African*

ACCEPTED MANUSCRIPT

Rift System. Geological Society, London, Special Publication 259, 77-93. DOI: 10.1144/GSL.SP.2006.259.01.08

Rooney TO, Hanan BB, Graham DW, Furman T, Blichert-Toft J, Schilling J-G 2012. Upper Mantle Pollution during Afar Plume - Continental Rift Interaction. Journal of Petrology 53, 365-389. DOI: 10.1093/petrology/egr065

Salem O, Visser JH, Dray M, Gonfiantini R. 1980. Groundwater flow patterns in the western Libyan Arab Jamahiriya evaluated from isotopic data. In: *Arid-Zone Hydrology: Investigations with Isotope Techniques*, IAEA, Vienna, 165–179

SanJuan, B., Michard, G., Michard, A., 1990. Origine des substances dissoutes dans les eaux des sources thermales et des forages de la région Asal-Goubhet (République de Djibouti). Journal of Volcanology and Geothermal Research 43, 333-352. DOI:10.1016/0377-0273(90)90060-S

Schoeller, H., 1962. Les Eaux Souterraines. Hydrologie dynamique et chimique, Recherche, Exploitation et Évaluation des Ressources. Masson et Cie, Paris.

Stadler S, Osenbrück K, Knöller K, Suckow A, Sültenfuss J, Oster H, Himmelsbach T, Hötzl H. 2008. Understanding the origin and fate of nitrate in groundwater of semi-arid environments. Journal of Arid Environments 72, 1830–1842. DOI: 10.1016/j.jaridenv.2008.06.003

ACCEPTED MANUSCRIPT

Tamers MA. 1967. Radiocarbon ages of groundwater in an arid zone unconfined aquifer. In: Stout GE (ed) Isotope Techniques in the Hydrologic Cycle. Geophysical Monograph Series Number 11, American Geophysical Union, Washington D.C., pp. 143-152. DOI: 10.1029/GM011p0143.

Teklemariam M, Beyene K. 2001. Geochemical monitoring of the Aluto-Langano Geothermal Field. Proceedings, Twenty-Sixth Workshop on Geothermal Reservoir Engineering Stanford University, Stanford, California, January 29-31, 2001, SGP-TR-168

Thorstenson DC, Parkhurst DL. 2004. Calculation of individual isotope equilibrium constants for geochemical reactions. Geochimica et Cosmochimica Acta 68, 2449–2465.

UNDP (United National Development Program) 1973. Geology, Geochemistry and hydrology of the East Africa Rift System within Ethiopia. Technical report prepared for the Imperial Ethiopian Government for the United Nations Development Programme, United Nations, New York, 227 pp.

Vengosh, A., 2014. Salinization and Saline Environments. In: Holland, H.D., K.K., Turekian, K.K., (eds), Treatise on Geochemistry 2nd Edition - Volume 11: Environmental Geochemistry, 325-378. DOI: 10.1016/B978-0-08-095975-7.00909-8

Vidal Ph, Deniel C, Vellutini PJ, Piguet P, Coulon C, Vincent J, Audin J. 1991. Changes of mantle source in the course of a rift evolution: The Afar Case. Geophysical Research Letters 18, 1913–1916. DOI: 10.1029/91GL02006

ACCEPTED MANUSCRIPT

Walvoord MA, Phillips FM, Stonestrom DA, Evans RD, Hartsough PC, Newman BD, Striegl RG. 2003. A Reservoir of Nitrate Beneath Desert Soils. Science 302, 1021-1024. DOI: 10.1126/science.1086435

WHO (World Health Organization) 2011. *Guidelines for drinking-water quality.* Fourth Edition, Geneva, Switzerland. http://apps.who.int/iris/bitstream/10665/44584/1/9789241548151_eng.pdf

ACCEPTED MANUSCRIPT

ACCEPTED MANUSCRIPT

Table 1. Sampling locations. T. Eh, depth, pH, EC, TDS, calculated partial pressure and hydrochemical types of the sampled waters.

	Samples	Latitude	Longitude	T (°C)	Eh (mV)	Depth (m)	DO (mg/l)	Filters depth (m)	EC (µS/cm)	TDS (mg/l)	$logP_{CO2}$	pH	Local categorie	Hydrochemical types
	Petit Bara Zone													
1	PK44	11.44416	42.81727	38	229	135	4.4	45-65; 85-110	956.9	666	-2.2	7.8	Alluvium - Petit Bara	Na-HCO3-Cl
2	PK48	11.43917	42.80333	36	238	133	4.3	40-64; 83-116	1099	688	-2.12	7.6	Alluvium - Petit Bara	Na-HCO3-Cl
3	PK50	11.43761	42.78342	38	231	92	4.1	60-90	1127	795	-2.29	7.9	Alluvium - Petit Bara	Na-HCO3-Cl
4	PK51	11.42322	42.76103	39	241	132	4.5	69-78; 100-118; 120-129	1204	811	-2.14	7.7	Alluvium - Petit Bara	Na-HCO3-Cl
5	Didjander	11.39842	42.75795	28	236	170	5.2	55-155	2876	1617	-2.57	7.9	Alluvium - Petit Bara	Na-Cl
6	Omar Jakka	11.3815	42.75508	38	228	160	3.4	100-130	2958	2015	-2.44	7.8	Alluvium - Petit Bara	Na-Cl
7	Naheel	11.35122	42.75233	39	234	155	6	100-140	6564	3668	-2.24	7.2	Alluvium - Petit Bara	Na-Cl-Mg
8	Kourtimaley ♠	11.33	42.67222	37	-	161	-	120-155	7731	-	-3.08	7.8	Central area	Na-Cl-Ca
	Grand Bara Zone													
9	Iskoutir	11.30153	42.69911	32	232	181	5.5	80-103 ; 136-160; 162-171	3258	2363	-2.82	7.8	Basalt - Grand Bara	Na-Cl-Ca-SO4
10	Dagahdamere	11.28267	42.6963	39	237	168	6.2	55-120; 130-155	4846	3484	-2.73	7.7	Basalt - Grand Bara	Na-Cl-Mg-Ca-SO4
11	Gor Galo	11.25814	42.71881	43	219	114	6.7	65-70; 80-90; 100-106	2871	1879	-2.42	7.8	Alluvium-Grand Bara	Na-Cl-SO4
12	Goroja ♥	11.24917	42.66389	42	-	90	-	60-85	6300	-	-2.66	7.8	Basalt - Central Grand Bara	Na-Cl-SO4
13	Hambocto F2	11.20783	42.67158	35	220	19	6.1	-	1896	1329	-1.96	7.3	Alluvium-Grand Bara	Na-Cl-Mg-Ca-HCO3
14	Hambocto F1	11.21311	42.66786	38	270	150	4	70-125	1464	988	-1.87	7.3	Basalt - Grand	Na-Cl-Mg-

ACCEPTED MANUSCRIPT

												Bara	Ca-HCO3
15	Doudoub Bololé F2	11.21308	42.65172	36	216	103	4.5	65-88	2337	1576	-2.36	7.6	Basalt - Grand Bara	Na-Cl-Mg-SO4
16	Doudoub Bololé F1	11.21483	42.64633	41	197	93	2.4	58-93	4143	3173	-2.45	7.5	Basalt - Grand Bara	Na-Cl-Mg-SO4
17	Awraoussa 1	11.19594	42.61178	36	217	195	4.8	114-152; 166-182	2692	1842	-2.65	7.8	Basalt - Grand Bara	Na-Cl-Mg-Ca-SO4
18	Gabla-galan	11.29444	42.58325	30	165	156	4.6	90-144	2200	1519	-3.07	8.4	Alluvium-Grand Bara	Na-Cl-HCO3-SO4
	Mouloud-Dadin Zone													
19	Mindil	11.20667	42.43175	36	205	150	4.6	65-120	2630	1824	-2.03	7.5	Basalt - Mouloud	Na-Cl-Mg-SO4
#	Mouloud 3	11.16525	42.50456	39	227	115	6.1	72-106	3035	2075	-2.19	7.5	Basalt - Mouloud	Na-Cl-Mg-SO4
21	Mouloud 4	11.1654	42.50442	39	230	140	5.7	100-122	2880	1965	-2.02	7.3	Basalt - Mouloud	Na-Cl-Mg-SO4
#	Dadin 3	11.14511	42.52781	34	262	139	4.7	36-50; 60-80; 96-134	1388	980	-1.72	7.4	Basalt - Dadin	Na-Cl-HCO3

♠ Closed after drilling in 1985 because of the high salinity of its groundwater; ♥ Closed after drilling in 1978 because of the high salinity of its groundwater.

ACCEPTED MANUSCRIPT

Table 2. Hydrochemical characteristics (in mg/l) of water samples in the study area and saturation index (SI) of selected minerals

	Site	Ca (mg/l)	Mg (mg/l)	Na (mg/l)	K (mg/l)	Li (mg/l)	NH_4 (mg/l)	HCO_3 (mg/l)	Cl (mg/l)	SO_4 (mg/l)	NO_3 (mg/l)	F (mg/l)	Br (mg/l)	B (mg/l)	Sr (mg/l)	♦SiO_2(aq) (mg/l)	NO_2 (mg/l)	IBE (%)	Calcite (SI)	Dolomite (SI)	Anhydrite (SI)	Halite (SI)
	Petit Bara Zone																					
1	PK 44	28.8	22.8	165.3	4.9	≤ DL	≤ DL	267.2	131.9	84.3	29.6	0.6	0.5	–	0.69	39.8	0.02	1	0.12	0.6	-2.28	-6.29
2	PK 48	26.8	22.7	151.6	4.1	0.02	0.01	347.8	100.1	65.7	12.4	0.83	0.41	–	0.54	40.1	0.01	-1	0.33	1.04	-2.42	-6.44
3	PK 50	24.9	22.2	187.7	4.4	0.04	≤ DL	352.9	147	77.9	17.7	0.71	0.72	0.06	0.57	41	≤ DL	-2	0.52	1.47	-2.4	-6.19
4	PK 51	23.1	21.1	222.9	4.3	0.01	≤ DL	307.9	189.1	88.9	14.8	0.78	0.85	0.15	0.53	40.6	0.03	1	0.23	1.18	-2.37	-6.01
5	Didjan Der	88	63.2	384	18.5	0.9	0.13	237.1	609.5	198	32.5	0.01	2.88	–	–	–	0.03	2	0.66	1.55	-1.7	-5.28
6	Omar Jakka	89.9	68.9	435.7	8.5	0.02	≤ DL	219	697.8	234	54.3	0.43	2.69	0.36	2.24	34.3	0.02	0	0.57	1.49	-1.61	-5.2
7	Naheel	215	231	852.5	11	0.2	0.43	95	1874	608	119	0.9	7.74	0.89	6.5	46.0	0.15	-1	-0.13	0.24	-1.1	-4.54
8	Kourtimaley ♠	368	165	1080	32	–	–	61	2410	572	122	–	–	–	–	–	–	-2	0.45	1.01	-0.92	-4.33
	Grand Bara Zone																					
9	Iskoutir	145.7	65.2	440.1	8.2	0.02	≤ DL	100.9	818.5	319	50.8	0.28	3.5	1.95	3.80	–	0.09	0	0.37	0.8	-1.33	-5.11
10	Dagahdamere	199.3	123	653	15.3	≤ DL	0.8	95	1272	487	62	0.09	5.29	0.22	6.71	37.4	0.21	0	0.39	1.04	-1.11	-4.8
11	Gor Galo	88.5	57.4	453	8.3	0.04	≤ DL	213.3	572.1	334	142	0.89	2.5	1.18	2.58	38.2	≤ DL	0	0.6	1.49	-1.38	-5.28
12	Goroja ♥	180	132	1180	24	–	–	122	1990	553	130	–	–	–	–	–	–	0	0.53	1.39	-1.1	-4.4
13	Hambocto F2	115	66.8	169.5	5	0.01	≤ DL	209.7	269.2	131	255.7	0.60	2.35	0.07	2.37	43.7	≤ DL	2	0.14	0.49	-1.68	-6
14	Hambocto F1	58.4	38.7	186	4.1	0.01	≤ DL	239.7	249.8	113	49.8	1.01	1.27	4.31	2.6	38.6	≤ DL	0	0.05	0.39	-1.94	-5.98
15	Doudoub Bololeh F2	71	61.9	327.5	7.7	0.02	≤ DL	166.1	517.2	240	55.1	0.68	2.09	0.34	2.38	32.8	≤ DL	0	0.19	0.76	-1.64	-5.43
16	Doudoub Bololeh F1	165	134.8	507.5	13.1	0.03	≤ DL	107.7	1120	419	59.1	0.61	4.13	0.37	4.27	29.4	≤ DL	-2	0.19	0.77	-1.17	-4.96
17	Awraoussa 1	116.9	65.9	321.2	11.7	0.04	≤ DL	140.8	519	295	71	0.64	2.59	0.48	2.46	35.7	≤ DL	2	0.49	1.18	-1.37	-5.45
18	Gabla-galan	36.2	50.3	382.5	7.9	0.04	0.13	235.1	356	193	247.5	0.39	2.26	0.11	0.94	28.7	≤ DL	2	0.56	1.82	-2.1	-5.41
	Mouloud Zone																					
19	Mindil	55.1	92.6	361.2	9.8	0.02	≤ DL	283.7	481.4	301	47.3	0.52	2.51	1.91	2.82	32.8	≤ DL	2	0.13	0.92	-1.72	-5.43
20	Mouloud 3	82.2	79.8	442.9	10.9	0.02	≤ DL	188.9	686.9	337	79.6	0.43	2.73	0.31	2.39	32.6	≤ DL	-1	0.17	0.78	-1.51	-5.2
21	Mouloud 4	96.5	92.2	377.3	8.3	0.03	≤ DL	177.5	625.5	329	75.8	0.62	2.56	–	–	32.4	≤ DL	1	0.06	0.56	-1.45	-5.31
22	Dadin 3	46.9	26.4	217.5	5.1	0.03	≤ DL	443.6	157.3	103	33.8	1.51	0.4	≤ DL	1.02	30.9	0.07	-1	0.29	0.77	-2.08	-6.1

♠ Closed after drilling in 1985 because of the high salinity of its groundwater; ♥ Closed after drilling in 1978 because of the high salinity of its groundwater;

DL: Detection Limit (DL(B) = 0.3 µg/l; DL(NO_2)= 1.6µg/l); IBE: Ionic Balance Error.; ♦ $SiO_2(aq) \equiv H_4SiO_4°$

ACCEPTED MANUSCRIPT

ACCEPTED MANUSCRIPT

Table 3. Isotope data of Bara groundwaters from this study and literature.

	Samples	$\delta^{18}O(H_2O)$ (‰ vs V-SMOW)	$\delta^{2}H(H_2O)$ (‰ vs V-SMOW)	Tritium (TU)	$\delta^{13}C(DIC)$ (‰ vs PDB)	$\delta^{13}C(CO_2)_{aq}$ ♠ (‰ vs PDB)	$A^{14}C$ (pmC)	^{14}C age ♣ (years BP)	$^{87}Sr/^{86}Sr$	$\delta^{15}N(NO_3)$ (‰ vs AIR)	$\delta^{18}O(NO_3)$ (‰ vs V-SMOW)	reference
						Petit Bara Zone						
2	PK 48	-1.10	-4.8	0.7 ± 0.5	-	-	-	-	-	-	-	This study
3	PK 50	-1.10	-4.8	< 0.6	-11.81	-18.2	-	-	0.70600	8.45	8.46	This study
3	PK 50	-	-	< 2.2	-11.60♣	-17.9	69.9±0.9	1061±107	-	-	-	BGR (1982)
3	PK 50	-1.29	-	7 ± 1	-11.60	-17.8	≤60	-	-	-	-	Fontes et al. (1980)
3	PK 50	-1.57	-	-	-11.69	-17.9	80.4±1.0	23±104	-	-	-	Fontes et al. (1980)
4	PK 51	-1.10	-5.0	< 0.6	-11.41	-17.7	-	-	0.70606	8.84	7.25	This study
6	Omar Jakka	-1.70	-11.0	1.2 ± 0.6	-10.78	-17.1	-	-	0.70610	8.15	11.13	This study
7	Naheel	-3.24	-24.5	-	-8.71	-14.4	-	-	0.70596	7.57	16.79	This study
						Grand Bara Zone						
9	Iskoutir	-	-	-	-	-	-	-	-	6.70	7.04	This study
10	Dagah Damer	-3.65	-24.8	-	-	-	-	-	0.70594	-	-	This study
11	Gor Galo	-2.82	-17.1	-	-9.67	-15.6	-	-	0.70662	6.53	9.43	This study
12	Goroja	-3.20	-19.6	< 2.2	-8.40	-14.4	17.2±1.1	8943±546	-	-	-	BGR (1982)
13	Hambocto F2	-1.80	-8.9	0.8 ± 0.7	-9.83	-15.9	-	-	0.70668	8.58	11.53	This study
14	Hambocto F1	-2.94	-16.8	-	-7.99	-13.9	-	-	0.70657	6.78	7.37	This study
15	Doudoubolole F2	-3.30	-21.4	< 0.6	-6.89	-12.7	-	-	0.70648	8.18	10.66	This study
16	Doudoubolole F1	-3.70	-24.8	< 0.6	-7.09	-13.5	-	-	0.70637	9.31	12.74	This study
16	Doudoubolole	-4.06	-32.0	< 4	-8.40	-14.8	27.6±2.7	6266±850	-	-	-	Fontes et al. (1980)
17	Awraoussa 1	-3.10	-18.8	< 0.6	-8.74	-15.3	-	-	-	7.70	12.03	This study
18	Gabla Galan	-1.90	-9.4	< 0.6	-6.85	-14.5	-	-	0.70556	11.35	10.59	This study
						Mouloud-Dadine Zone						
19	Mindil	-3.90	-25.5	< 0.6	-10.75	-17.0	-	-	0.70647	9.24	10.09	This study
20	Mouloud 3	-3.40	-21.5	< 0.6	-10.31	-16.5	-	-	0.70613	8.47	11.16	This study
	Mouloud 5	-3.60	-21.3	-	-	-	-	-	-	-	-	Aboubaker et al. (2013)
20	Mouloud 3	-3.05	-20.1	< 2.1	-9.50	-15.9	49.6±0.8	2246±134	-	-	-	BGR (1982)
21	Mouloud	-3.93	-32.0	<4	-10.79	-17.0	52.2±2.5	3085±406	-	-	-	Fontes et al. (1980)
22	Dadin 3	-2.40	-1.3	< 0.6	-12.21	-18.5	-	-	0.70694	6.47	7.15	This study
	Dadin 6	-2.50	-1.2	-	-	-	-	-	-	-	-	Aboubaker et al. (2013)

ACCEPTED MANUSCRIPT

- not measured or not calculated

♠ $\delta^{13}C$ of aqueous CO_2 was calculated by PHREEQCI software and *iso.dat* database (Parkhurst and Appelo 2015).

♥ Corrected with the IAEA method

♣ Based on data from Fontes et al. (1980)

ACCEPTED MANUSCRIPT

ACCEPTED MANUSCRIPT

Figure 1

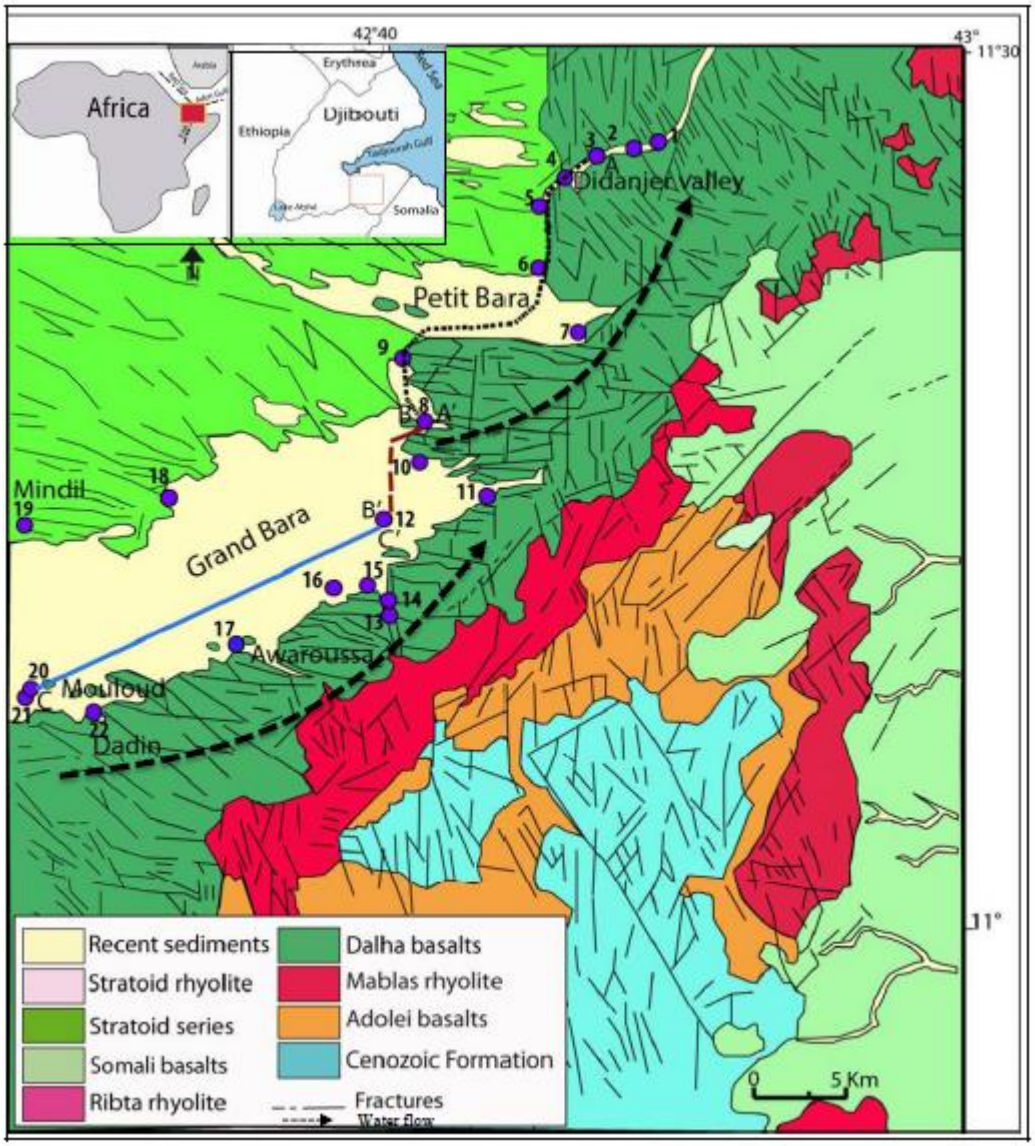

ACCEPTED MANUSCRIPT

Figure 2

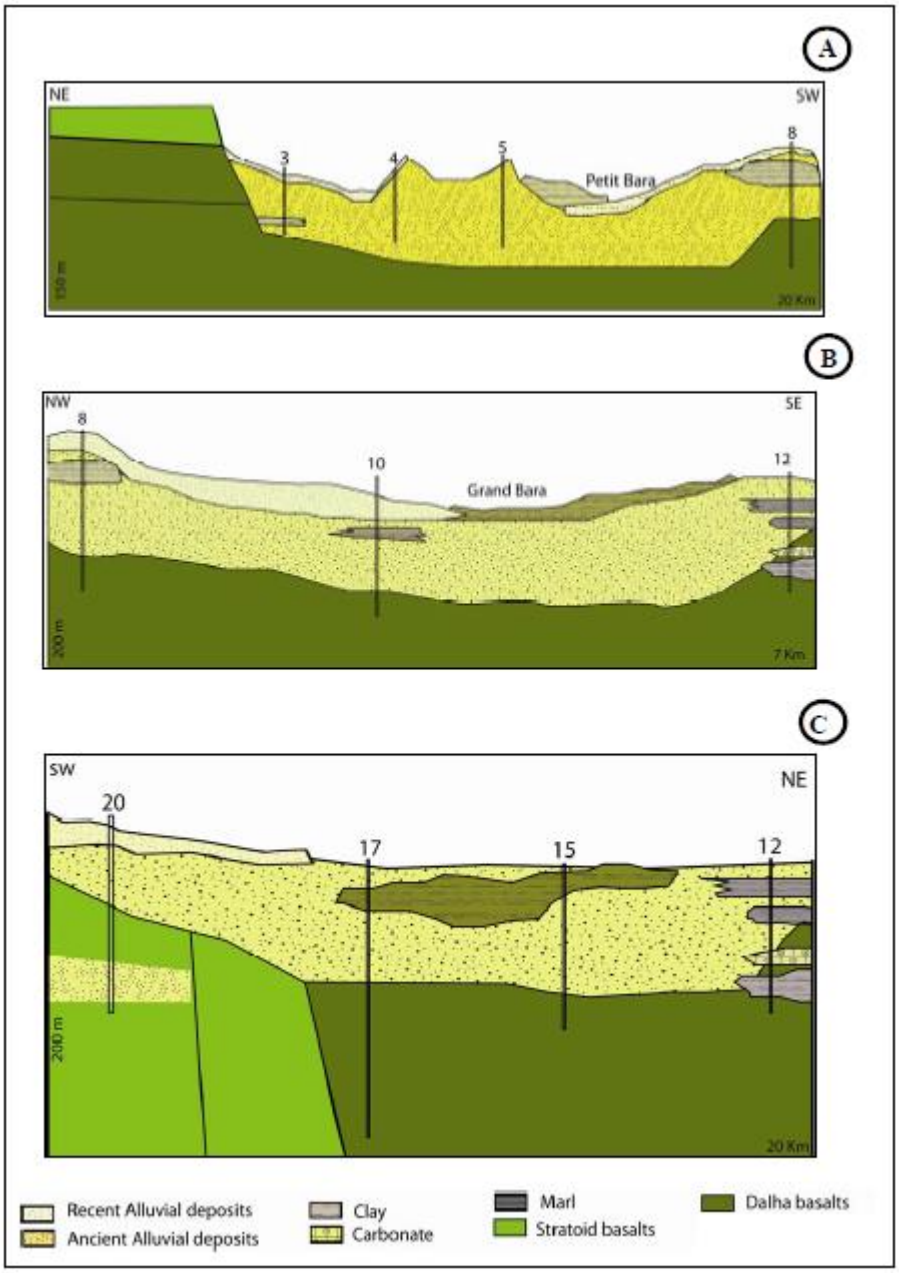

ACCEPTED MANUSCRIPT

Figure 3

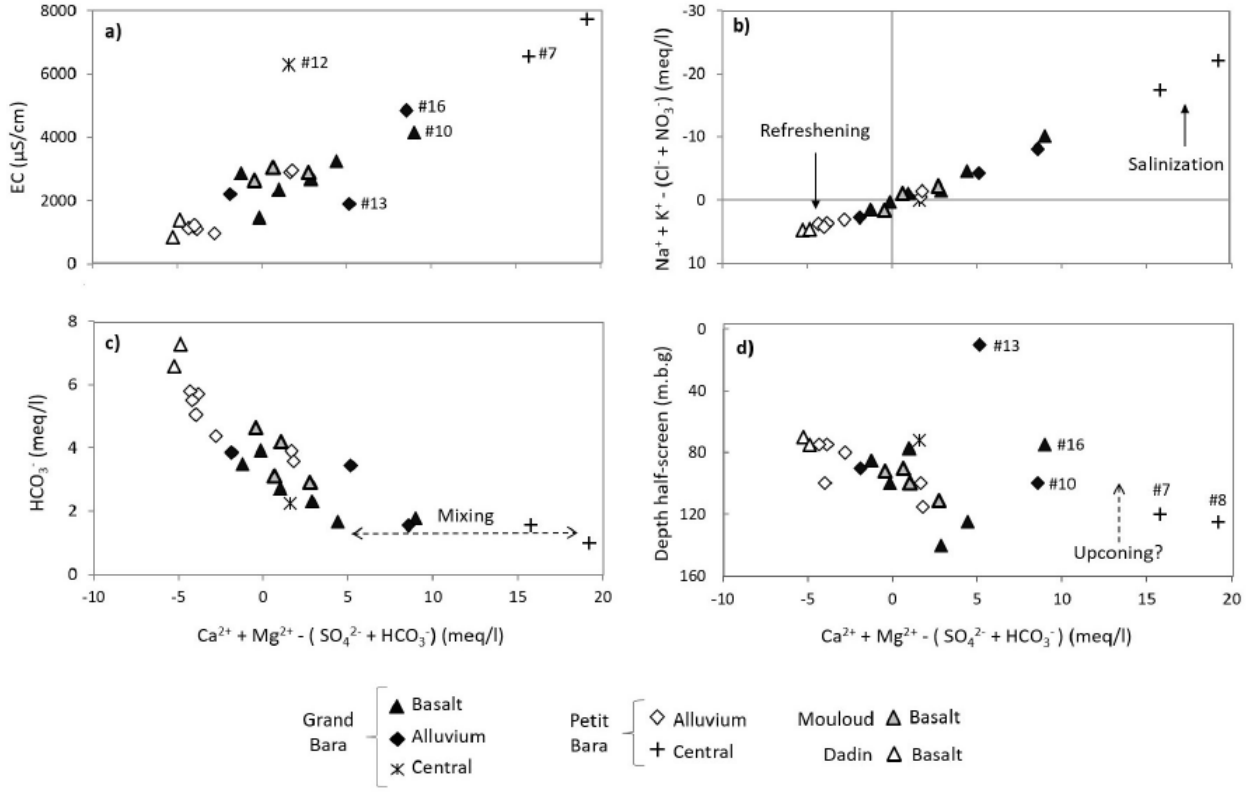

ACCEPTED MANUSCRIPT

ACCEPTED MANUSCRIPT

Figure 4

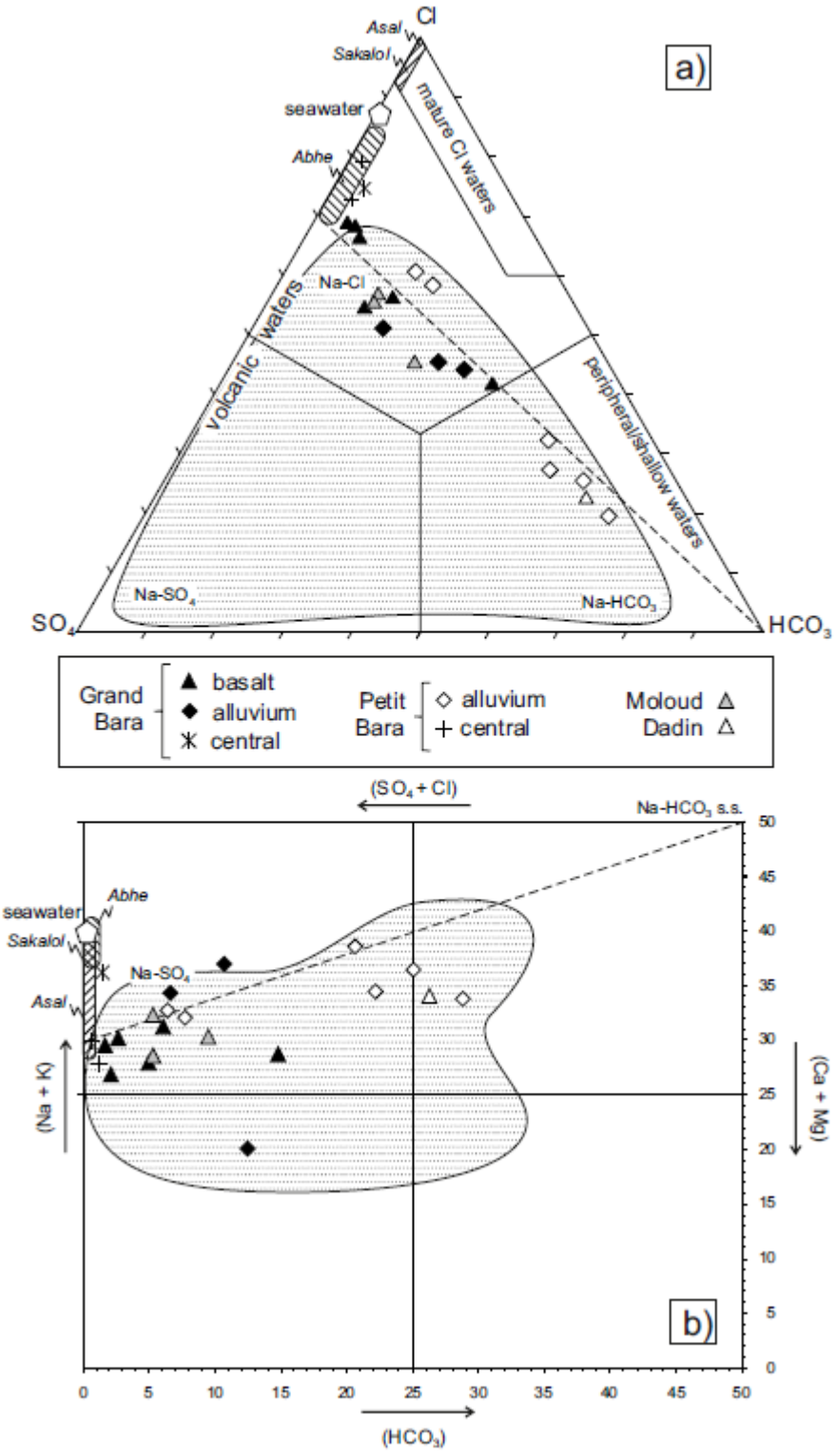

ACCEPTED MANUSCRIPT

Figure 5

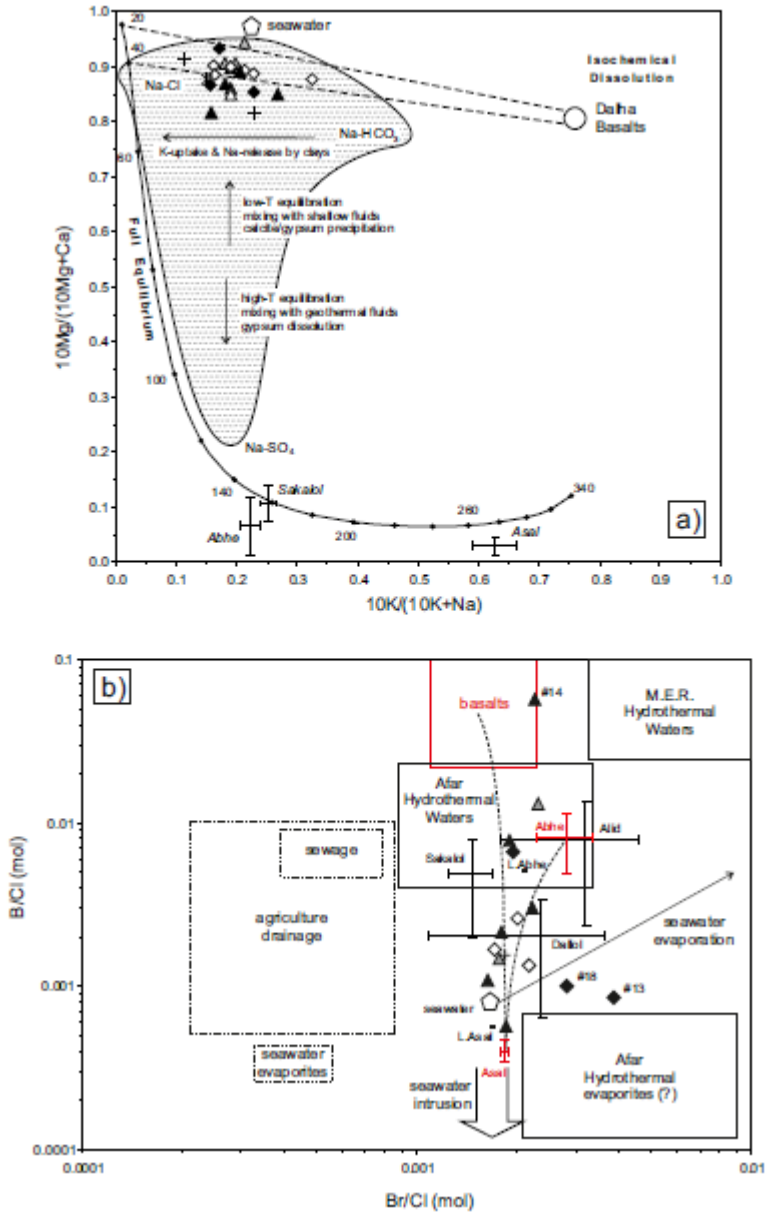

ACCEPTED MANUSCRIPT

Figure 6

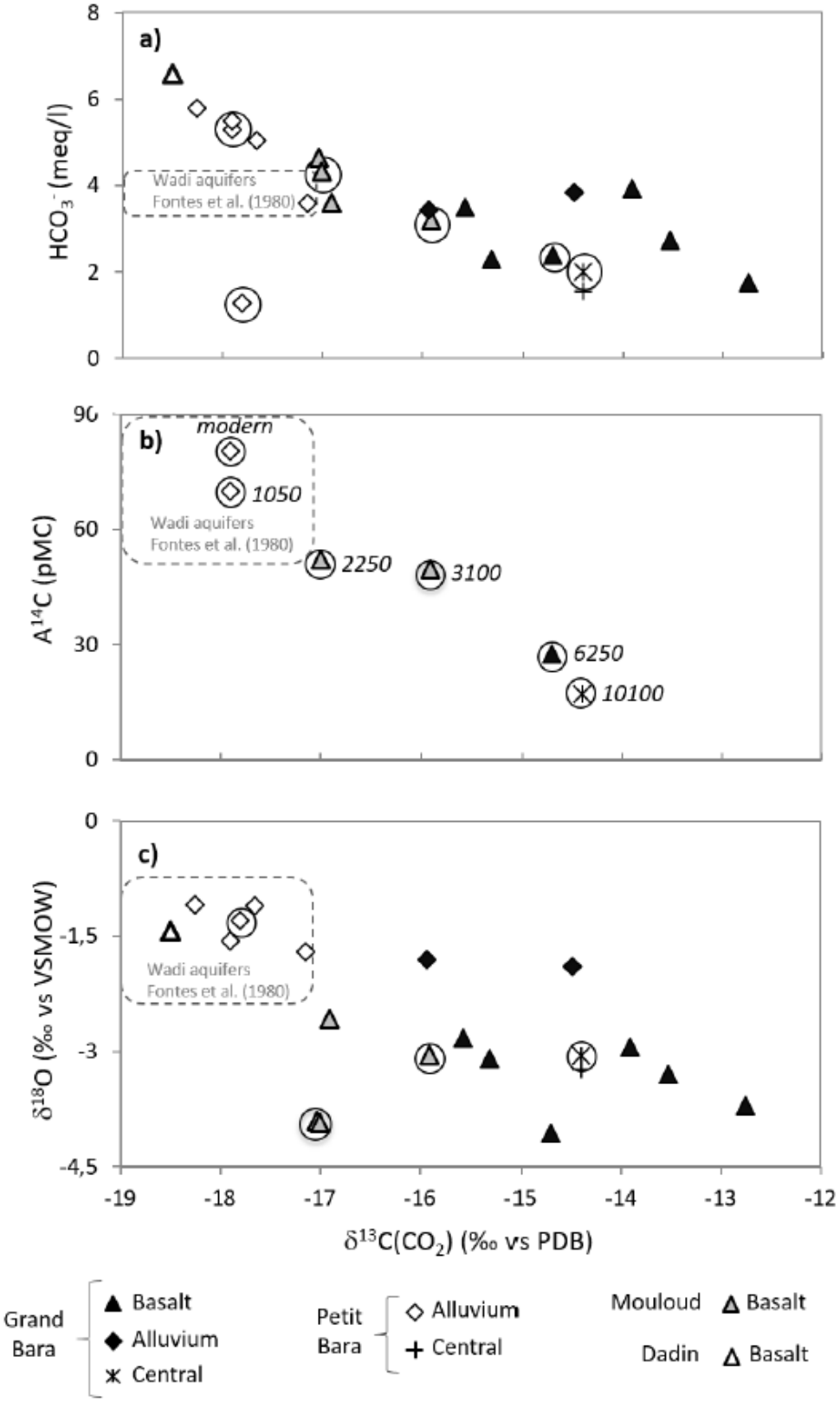

ACCEPTED MANUSCRIPT

Figure 7

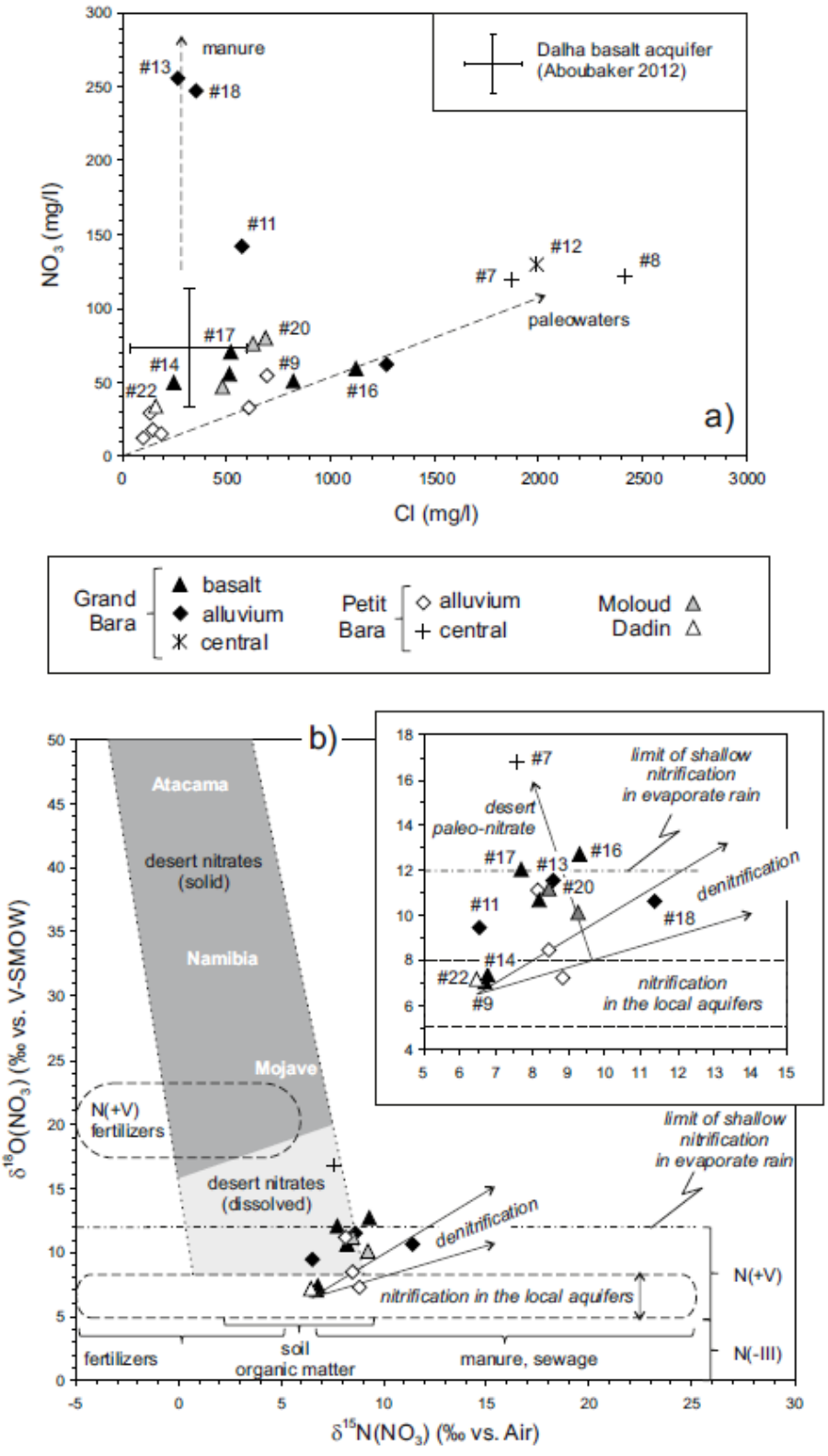

ACCEPTED MANUSCRIPT

Figure 8

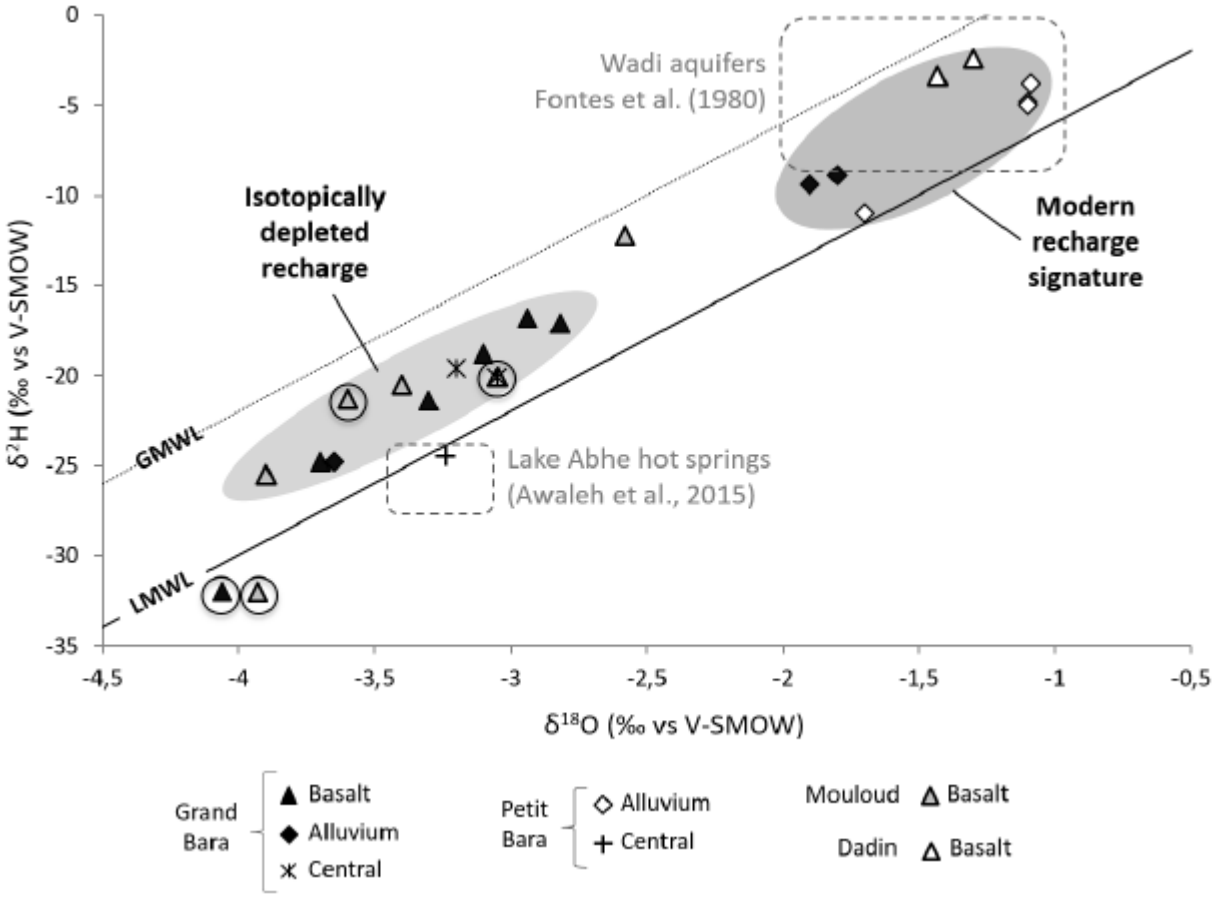

ACCEPTED

ACCEPTED MANUSCRIPT

Figure 9

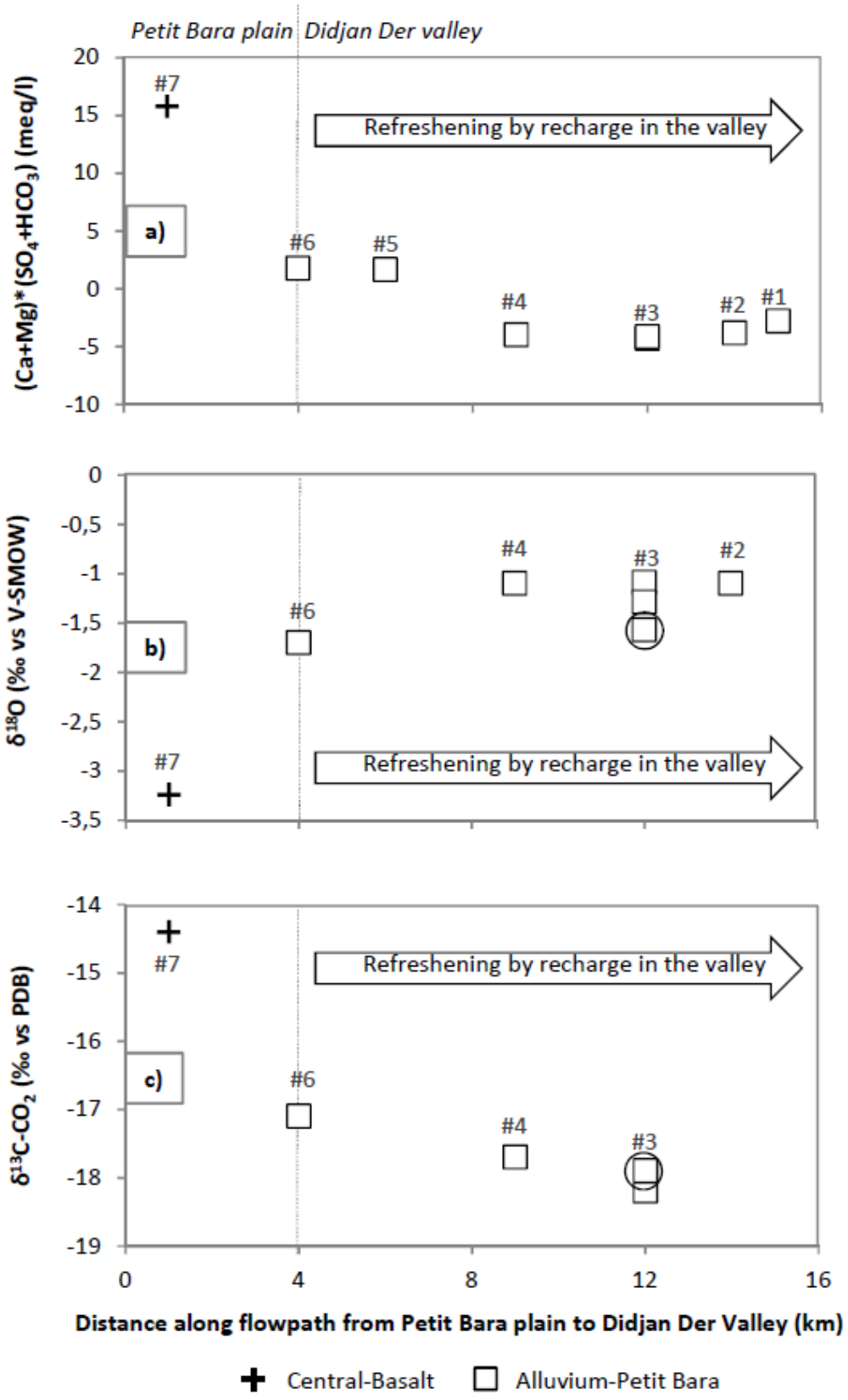

ACCEPTED MANUSCRIPT

Figure 10

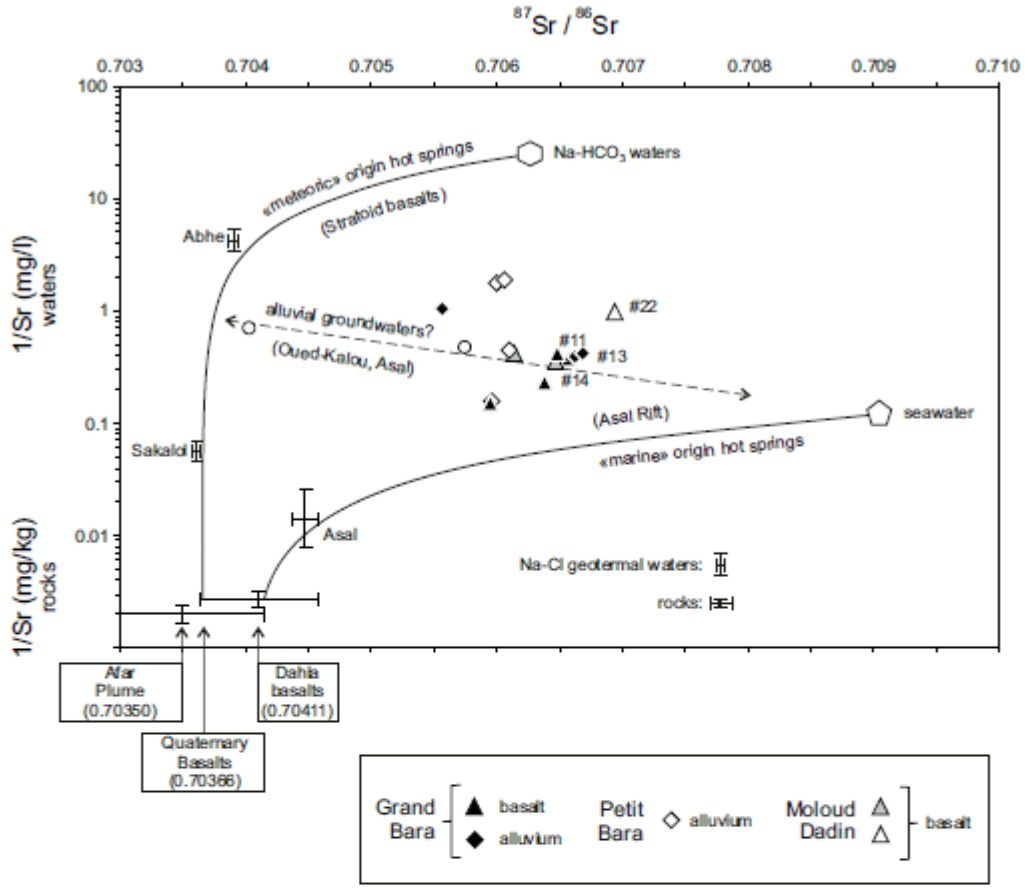

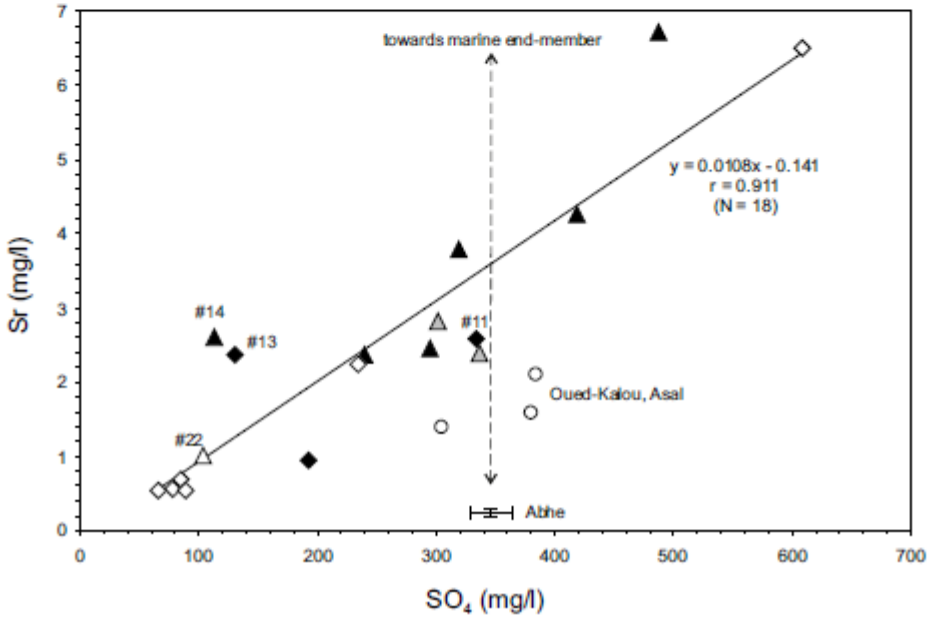

ACCEPTED MANUSCRIPT

Highlights

- Investigating an alluvium-basaltic aquifer system in arid eastern Africa
- Groundwater flow pattern and mixing revealed by geochemistry and isotopes
- Consistent recharge from wadis and downward circulation to the basalts
- Absence of a deep volcanic CO_2 contribution to basalt groundwater
- Soil, manure and caliche nitrate sources evidenced by isotopic nitrate

ACCEPTED MANUSCRIPT